ACI Research Paper #03-2021

International Trafficking in Persons and Global Health Security: Evidence From Two Modern Pandemics

Lucas SHEN

March 2021

Please cite this article as:

Lucas Shen, "International Trafficking in Persons and Global Health Security: Evidence From Two Modern Pandemics", Research Paper #03-2021, *Asia Competitiveness Institute Research Paper Series (March 2021)*

International Trafficking in Persons and Global Health Security: Evidence from Two Modern Pandemics

Lucas Shen*

March 2021

Abstract

This paper exploits cross-country differences in coastline distances as a measure of porosity to estimate the relative risk of trafficking in persons (TIP) inflows, finding smoking gun evidence that countries with a higher risk of TIP inflows have more cases per population during the modern pandemics. Institutional and health factors mainly influence the results through the TIP channel, with their effects largely muted in the second stage. In addition, migration flows—including flows from the pandemic source country—have no estimated effect on local numbers conditional on the instrumented risk of TIP inflow.

Introduction

In the wake of the 2020 COVID-19 pandemic, understanding how travel restrictions and mobility influence the spread of epidemics is of great interest (e.g. Ferguson et al. 2006; Chinazzi et al. 2020; Fang et al. 2020; Kraemer et al. 2020). In this paper, I focus on the cross-country link between the risk of human trafficking inflow into countries and the severity of the two most recent episodes of pandemics—the H1N1 and the COVID-19 pandemic. These flows of trafficked persons are potentially important since trafficked persons constitute part of undocumented cases and are thus linked to the spread of epidemics (Li et al., 2020; Long et al., 2020), and trafficked persons are themselves of interest, being a particularly vulnerable group

*Comments welcome to: lucas@lucasshen.com. Click here for latest draft. I am grateful to comments and insights from an anonymous marine engineer and Giovanni Ko. For brevity, both countries and territories are referred to as "countries". Interpretations are those of the author and do not necessarily indicate concurrence by any institutional affiliation. All errors are my own.

during pandemics (Page et al. 2020; Greenaway and Gushulak 2017; Wickramage et al. 2018; UNODC [United Nations Office on Drugs and Crimes] 2020a).

While little direct evidence exists between the cross-country link of TIP (trafficking in persons) and the spread of pandemics, I begin with two motivating facts from the two modern pandemics. First, Italy became one of the hardest-hit countries after China itself, the source of the COVID-19 pandemic, and various theories have been proposed for their high numbers, including an aging population and just plain bad luck (Agence France-Presse [AFP] 2020; Simon 2020). Another potential explanation lies with trafficking networks in Italy exploiting foreign victims, who originate primarily from African countries, Eastern European countries, and China, where textile factories in particular "exploit Chinese and other victims in Milan, Prato, Rome, and Naples", and Chinese trafficking networks "force victims to work in apartments and in massage parlors" (U.S. Department of State 2019, p. 259). These unregistered workers, of which Italy has an estimated 1.5 million (U.S. Department of State 2019, p. 259), may increase the risk of local epidemics since it is difficult for authorities to trace and screen them.

Second, the H1N1 virus originated from Mexico in 2009, and one country that was hardest hit is Mexico's bordering neighbor to the North, the U.S., where their confirmed number of cases by the third month into the pandemic stands at (almost exactly) the 95th percentile, and this has to do with the geographical proximity and economic activity between the two countries, including the persistent illegal activity of migrant smuggling (Spener 2004; Gathmann 2008). A less obvious anecdote comes from Europe in Switzerland, where the CTDC (Counter-Trafficking Data Collaborative) (2017) documents a direct trafficking corridor between Switzerland and Mexico. In particular, Switzerland's 2009 profile states that the majority of its identified trafficking victims originated from Eastern Europe (50 percent), and the next largest source comes from Latin America (27 percent, U.S. Department of State 2009, p. 271). By the third month (June) into the H1N1 pandemic, Switzerland has the lowest population but highest confirmed cases per population out of its bordering neighbors.

To provide the first and preliminary evidence of the effect of trafficking in persons and pandemic severity, I use human trafficking indicators to measure relative risk of TIP (trafficking in persons) inflows to outflows of trafficked persons (Frank 2013), and link this measure to the confirmed number of cases per population in the two pandemics. Figures I and II illustrate this correlation for the H1N1 and the COVID-19 pandemics.

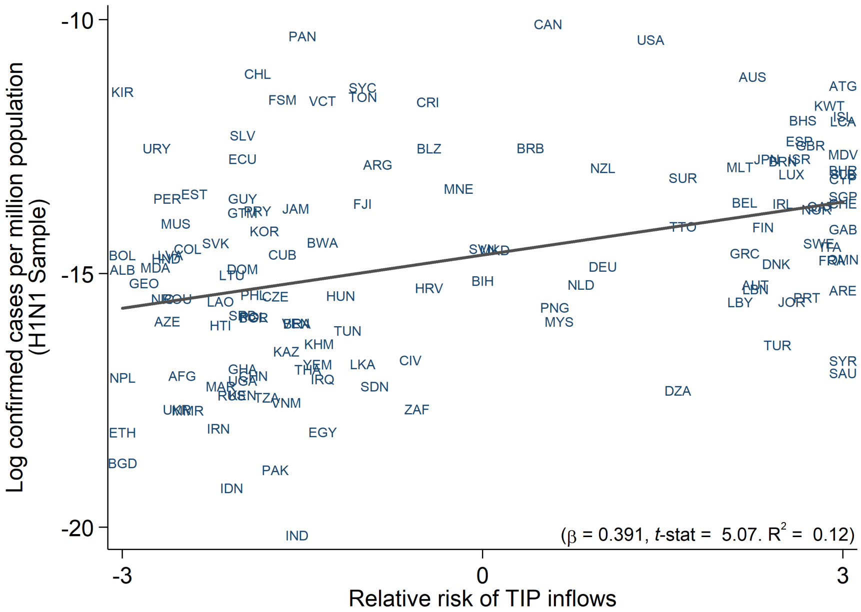

Figure I: OLS Relationship: Trafficking and the H1N1 Pandemic

Notes—Scatterplot of the log confirmed cases per million population by the end of the 3rd month into the H1N1 pandemic (June 2009), against the relative risk of international trafficking in persons flow measure defined in equation (1)—higher number indicates higher inflow risk. The highest 5 percentile in log confirmed cases per million population omitted in the graph. Estimated β coefficient, its t-statistic, and the R^2 come from a simple linear regression.

Since the relative risk of TIP inflows is unlikely to be exogenous, I use coastline distance to land area ratio as a measure of *porosity* and use this as an instrument for countries relative TIP inflows, on the premise that longer coastlines are more porous and thus have higher risk of trafficking inflows. One immediate connection between coastlines and trafficking has to do with how trafficking in international waters is hidden and difficult for authorities to detect (UNODC [United Nations Office on Drugs and Crimes] 2016, p. 104). For example, Bangladesh's 2018 profile states that trafficking victims transited through various land and sea routes (U.S. Department of State 2018, p. 91). The magnitude of crossings by sea routes is non-trivial. Djibouti's profile in 2017 states that "more than 117,000 people embarked on the sea crossing from the Horn of Africa to Yemen" (U.S. Department of State 2018, p. 168). For Italy, they "received 23,370 irregular arrivals by sea" in just 2018 alone (U.S. Department of State 2019, p. 259).

The two-stage least-squares (2SLS) estimates using the coastline instrument suggest that countries with a higher relative risk of TIP inflows face a higher number of confirmed cases per population. Controlling for gravity-type variables to the source country the pandemic barely attenuates the estimates. This approach also provides three further insights. First, cross-country differences in institutions and health measures mostly affect local confirmed numbers only indirectly through the channel of trafficking flows. This largely reflects how flows of trafficked persons closely resemble flows of migration—from less to more developed areas. Second,

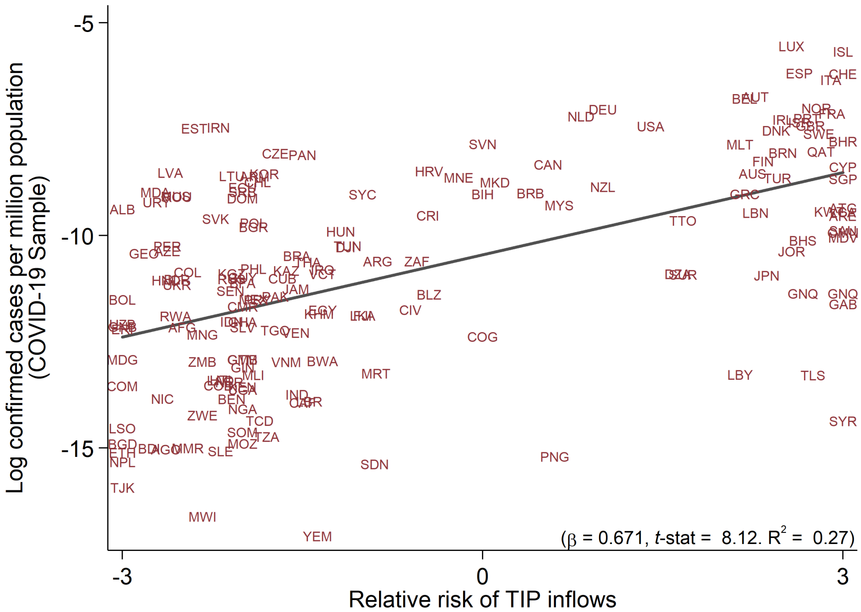

Figure II: OLS Relationship: Trafficking and the COVID-19 Pandemic

Notes—Scatterplot of the log confirmed cases per million population by the end of the 3rd month into the COVID-19 pandemic (March 2020), against the relative risk of international trafficking in persons flow measure defined in equation (1), higher number indicates higher inflow risk. The highest 5 percentile in log confirmed cases per million population omitted in the graph. Estimated β coefficient, its t-statistic, and the R^2 come from a simple linear regression.

it turns out that controlling for the number of tests conducted produces the most precise estimate, which is consistent with the need for higher testing numbers. Third, with the instrumented relative TIP inflowmeasure, both the flow and stock of migrants (regular and irregular), and in particular the regular migration inflow from the pandemic source country, are no longer positively associated with local confirmed numbers. Countries with larger export dependence on tourism however, face consistently higher numbers.

To further test the extent of a causal interpretation, I perform placebo regressions with fatality as the dependent variables and show that the results are not an artifact of the relative TIP inflowmeasure capturing differences in institutions and healthcare infrastructure. I also use data from drug inflows and seizures as alternative instruments, exploiting the connection drug and human trafficking routes (UNODC [United Nations Office on Drugs and Crimes] 2011, 2018b; Slack and Campbell 2016). These measures provide some direct support for the exclusion restriction of the coastline instrument. The findings are also robust to the inclusion of various sets of institutional, health, international mobility, and geographical factors, though the results are least robust with the log health expenditure per capita control. A further caveat to the results is that the exclusion of (Northern and Western) European countries increases the standard errors considerably (approximately twice), even though the estimates remain similar and statistically different from zero (Figure A2).

This paper provides preliminary smoking gun evidence on the effect of illegal flows of persons on pandemic severity. While there is some basis for causal interpretation, the results should be interpreted with caution since the relative risk of TIP inflow measure constructed from trafficking indicators is bound to capture only a small variation in the true and hidden prevalence of trafficking in persons.[1] Another implication is that a "pure" definition of trafficking is difficult since many types exist, and are closely linked to movements of irregular migrants. Large transregional trafficking operations for example are typically involved in border crossings that always require travel documents, making it difficult to separate trafficked persons from other migrants (UNODC [United Nations Office on Drugs and Crimes] 2014, p. 14). Hence the results in this paper may well be capturing the broad flows of irregular migrants, including refugee and asylum-seekers rather than just trafficked persons. In this sense, a related contribution of the paper is on how irregular migrants, including trafficked persons, are particularly vulnerable groups in society during a pandemic crisis, and thus require concerted tracing efforts and protection measures (Page et al. 2020; Greenaway and Gushulak 2017; Wickramage et al. 2018; UNODC [United Nations Office on Drugs and Crimes] 2020a).

This paper contributes to the existing literature on human trafficking (Akee et al. 2014; Bales 2007; Cho et al. 2013; Hernandez and Rudolph 2015; Jakobsson and Kotsadam 2013), which largely focus on the determinants of trafficking patterns. This paper is also related to contemporaneous studies on how travel restrictions and mobility influences the spread of COVID-19 (Chinazzi et al. 2020; Fang et al. 2020; Kraemer et al. 2020; Li et al. 2020; Kuchler et al. 2020); and past literature on migration and global health security in the context of the 2015 Zika epidemic (Bogoch et al. 2016), the 2003 SARS epidemic (St John et al. 2005), the H1N1 pandemic (Khan et al. 2013), and the MERS epidemic (Williams et al. 2015). More generally, this paper is related to studies connecting economic activity and the spread of viruses (Adda, 2016; Oster, 2012).

The next section provides additional motivating facts. Section III outlines the two-stage least-squares approach and the main data sources. Section IV and V presents the OLS and 2SLS least squares. Section VI presents the robustness tests. Section VII concludes.

[1] Limited numbers of *identified* victims and few convictions of traffickers do not imply low activity of trafficking. One indication of the prevalence of trafficking is that "victims trafficked from subregions with low detection and conviction rates are found in large numbers in other subregions" (UNODC [United Nations Office on Drugs and Crimes] 2018a, p.8).

(a) Mexico to Switzerland (H1N1)

(b) China to North Macedonia (COVID-19)

(c) North Macedonia to Italy (COVID-19)

Figure III: Illustration of Trafficking Corridors

Notes—Screenshots from the global trafficking corridor visualizer from the CTDC (Counter-Trafficking Data Collaborative) (2017) website: `https://www.ctdatacollaborative.org/map?type=corridor`. These observed corridors are constructed using reported numbers of trafficking cases.

Smoke, from a Smoking Gun?

While there is no extant literature on the effect of human trafficking on pandemics (to the best of my knowledge), some basic leads suggest such a potential link. First, in the early stages of the COVID-19 pandemic which began in January 2020, Italy became badly hit by the outbreak compared to its European counterparts. By the end of the 1st week of March, Italy had 5,883 confirmed cases, compared to its bordering neighbors at the same time: Austria (81), France (949), Slovenia (12), and Switzerland (268). Spain, who shortly had a similar crisis, had only 525 cases at this same time.[2] Italy's COVID-19 numbers became a puzzle in the global me-

[2] `https://www.worldometers.info/coronavirus/`.

dia, with various theories suggested, including having an aging population, a high degree of intergenerational interaction that fostered transmission to vulnerable groups in society, and just plain bad luck (Agence France-Presse [AFP] 2020; Simon 2020).[3]

The rest of this paper focuses on the singular channel of trafficking inflow and confirmed cases. Figure III shows three selected trafficking corridors identified by the CTDC *(Counter-Trafficking Data Collaborative)*.[4] Panel B illustrates that one of China's main outflow of trafficking is to North Macedonia, and Panel C in turn shows that one of North Macedonia's main outflow of trafficking is to Italy. For Spain on the other hand (corridor not shown), one of its main inflow sources of trafficking comes from Bulgaria, which borders North Macedonia, a major point of transit in human trafficking (U.S. Department of State 2019). The report states that "foreign victims transiting North Macedonia are subjected to sex trafficking and forced labor in construction and agricultural sectors in Southern, Central, and Western Europe" (U.S. Department of State 2019, p. 360).[5]

A second and more direct anecdote comes from Switzerland during the earlier 2009 H1N1 pandemic. Other than the United States, Mexico's most prominent observed trafficking corridor is to Switzerland (Panel A of Figure III), and Switzerland had 609 confirmed cases near the end of the pandemic compared to its bordering neighbors: Austria–192, France–880, Germany–9,213, Liechtenstein–5, and Italy–1,238. To put the numbers in perspective, by the fourth month into the pandemic in July 2009, Switzerland has the lowest population out of these countries but the highest confirmed cases per population.[6]

[3] In Italy's case for the COVID-19 pandemic, Kuchler et al. (2020) offer an alternative explanation. They use the social connectedness index from Facebook and find that Italian provinces with higher connectedness to Lodi—which contains Codogno, the town where the earliest local cases of COVID-19 were detected—have higher confirmed cases per population. The underlying premise is also about movement, where travel patterns follow social networks.

[4] `https://www.ctdatacollaborative.org/map?type=corridor`.

[5] Confirmed cases per million population by 3rd month (March) of COVID-19 pandemic, in descending order: Italy–98, Switzerland–33, France–14, Spain–11, Austria–9, Slovenia–6.

[6] Confirmed cases per million population by 3rd month (June) of H1N1 pandemic: Switzerland–8, Germany–5, France–4, Italy–2, and Austria–2.

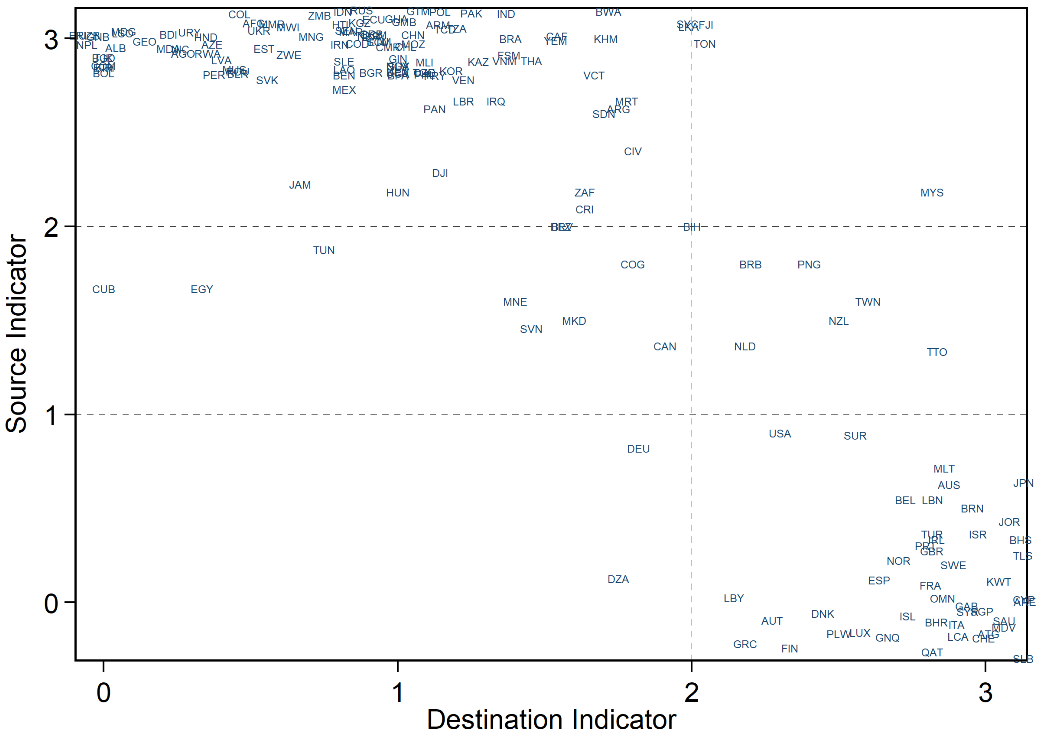

Figure IV: Risk of Trafficking Inflows (Destination) and Outflows (Source)

Notes—Scatterplot of countries source of human trafficking indicator against destination of human trafficking indicator, averaged over the years 2000–2011, with both measures taken directly from Frank (2013), originally from the U.S. Department of State (2001) annual TIP reports. Numbers should not be read off the graph literally as some random noise have been added to the top left and bottom right of the plot for the sake of visual articulation. Table A1 reports the exact records.

Data and Empirical Design

A. Human Trafficking Indicators

The measure of TIP in this paper is the relative risk of TIP inflow, the degree to which a country is a point of destination as opposed to a point of source in the international trafficking scene (2001–11):

(1) Relative TIP inflow = Mean(destination indicator) − Mean(source indicator).

The direct data source is Frank (2013)'s Human Trafficking Indicators dataset which covers macroscopic patterns in human trafficking and government efforts for 179 countries over the span of 12 years (2001–11). The Frank (2013) dataset uses the 2001–11 Trafficking in Persons (TIP) reports from the U.S. Department of State's Office to Monitor and Combat Trafficking in Persons (TIP Office).[7]

The destination indicators and source indicators, taken directly from Frank (2013), are constructed as follows. For each country in each year, there is a destination, source, plus transit indicator going from 1 to 3 depending on the order

[7] Their inaugural TIP report came after the *Victims of Trafficking and Violence Protection Act* was passed in Congress in 2000.

in which a country's profile mentions *destination*, *transit*, or *source* of trafficking. Returning to the example of Switzerland in 2009, the Switzerland profile begins by stating that the country is "primarily a destination and, to a lesser extent, a transit country for women and children trafficked for the purposes of commercial sexual exploitation and forced labor" (U.S. Department of State 2009). So for Switzerland in the year 2009, the destination indicator is recorded as 3 since 'destination' is mentioned first, the transit indicator is recorded as 2 since 'transit' is mentioned second, and the source indicator is recorded as 0 since it was never mentioned; if it had been mentioned and mentioned last the source indicator would be 1.

Figure IV shows the scatterplot of countries based on their reported prevalence of trafficking inflows (destination) and outflows (source). Countries on the top left are those countries implied to be most at risk of TIP outflow (e.g. Georgia (GEO), Uruguay (URY)), while those countries on the bottom right are those that are most at risk of TIP inflow (e.g. Italy (ITA), Switzerland (CHE)). Only a few countries are of relatively equal risk of inflow and outflow of TIP, such as Canada. Most countries fall in either the top left or bottom right sections.

The measure for the relative risk of TIP inflow uses both information on inflows *and* outflows since the coding of the data itself is done with one in relation to the other. The relative TIP inflowmeasure is increasing in the implied relative risk of human trafficking inflow, and has considerable variation with a mean of -0.36 and a standard deviation of of 2.14, the minimum and maximum are by construction -3 and 3, with negative figures implying that the country is of greater risk of facing outflow than inflow of TIP. Table A1 lists the recorded relative TIP inflowtogether with country codes and region.[8]

B. Confirmed Cases and Deaths of Pandemics

The dependent variable in the main results is the log of confirmed cases, per million population, by the 3rd month into the two recent pandemic episodes: the H1N1 pandemic (also known as Influenza A or the swine flu) and the 2019/20 COVID-19 pandemic. The H1N1 data comes from the 2009 swine flu pandemic tables, which includes confirmed cases and deaths in 2009 from April till August when the pandemic subsided and the ECDC slowed down on its reports.[9] COVID-19

[8] Using just the mean of the destination indicator alone, on the other hand, has a mean of 1.6 and a lower standard deviation of 0.98. The conclusion however, does not rely on the particular measure of trafficking inflow as defined in equation (1), since the conclusions are essentially the same when using the destination indicator alone (Figures A1).

[9] Available at `https://en.wikipedia.org/wiki/2009_swine_flu_pandemic_tables`. The num-

numbers come from the Johns Hopkins University.[10]

As a necessary assumption, I assume zero cases for those observations not observed. This problem is most severe in the first month, and gradually becomes less of an issue. Of the 301 country-pandemic episode observations in the most inclusive baseline regressions, 277 observations are missing in the first month (92.0%), 232 observations are missing by the second month (77.1%), and 76 observations are missing by the third month (25.2%).

C. Coastline Distance to Land Area as an Instrument

The main subject of investigation in this paper is the cross-country link between human trafficking and the severity of pandemic. The structural equation of interest is:

$$y_{id} = \alpha + \delta_d + \gamma_i + \beta(\text{Relative TIP inflow})_i + \boldsymbol{X}_i + \boldsymbol{G}_{id} + \varepsilon_{id}, \quad (2)$$

where y_{id} is the log of confirmed cases for country i in pandemic episode d by the 3rd month per million population. δ_d is the dummy for the COVID-19 pandemic (with H1N1 pandemic the omitted category), capturing epidemiological differences. γ_i includes 13 region dummies.[11]

β is the main coefficient of interest, capturing the effect of the relative risk of trafficking in persons on the confirmed numbers per population. $\boldsymbol{X}_i$ and $\boldsymbol{G}_{id}$ are covariates for country characteristics and a gravity-type linkage to the source country of the virus. G_{id} include dummies for whether countries share a common language with the source, whether they share a common border, whether they have an existing PTA (preferential trade agreement), and a measure of population-weighted distance to the source country of pandemic. These gravity-type data and the region dummies come from Gurevich and Herman (2018).[12]

Since a country's flows of trafficking in persons and its pandemic episode are both highly likely correlated with the quality of its institutions and economic connectivity, a direct cross-country comparison of the effect of trafficking in persons inflow and pandemic severity in equation (2) may well be biased upwards. On the

bers originate from the World Health Organisation (WHO) and The European Centre for Disease Prevention and Control (ECDC).

[10] Available at https://github.com/CSSEGISandData/COVID-19. Their data repository draws from numerous sources including the WHO, ECDC, and other government organizations like the CDCs of China, Taiwan, and the US.

[11] The 13 regions are Africa, Carribbean, Central America, Central Asia, East Asia, Eurasia, Europe, Middle East, North America, Pacific, South America, South Asia, and Southeast Asia. Table A1 lists the countries and their corresponding regions.

[12] Mexico for the H1N1 sample and China for the COVID-19 sample are dropped.

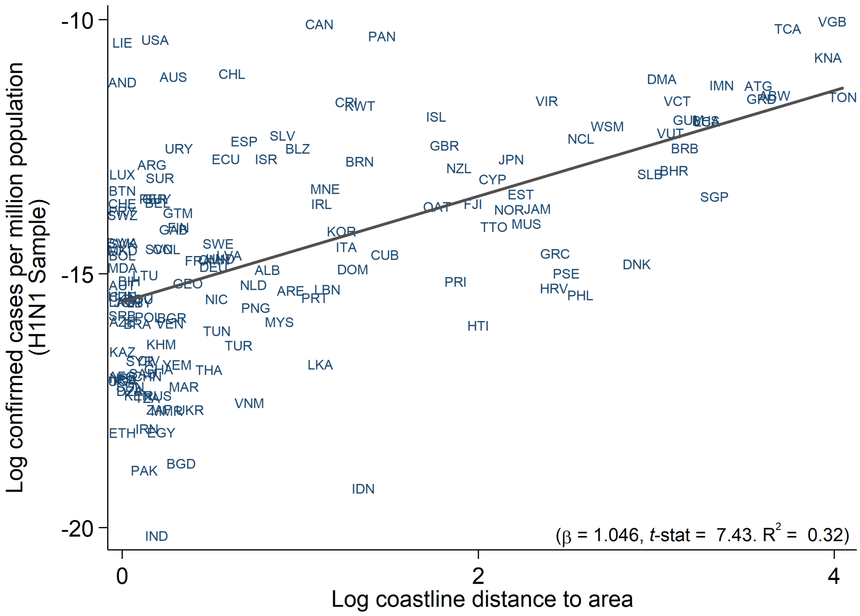

Figure V: Reduced-Form Relationship: Trafficking and the H1N1 Pandemic

Notes—Scatterplot of the log confirmed cases per million population by the end of the 3rd month into the H1N1 pandemic (June 2009), against log coastline distance to area. The highest 5 percentile in log confirmed cases per million population and coastline distance to area omitted in the graph. Estimated β coefficient, its t-statistic, and the R^2 come from a simple linear regression.

other hand, the opacity of true trafficking flows implies that the relative TIP inflowmeasure suffers from measurement error, which creates an attenuation bias. For example, both Italy and Switzerland have virtually the same relative TIP inflowmeasure in 2001–11 (3.9 and 4, respectively), but the true flows of trafficking in these two countries likely differ to a far greater extent than their relative TIP inflowmeasures suggest.

To handle the likely endogeneity of the relative risk of TIP inflow, including errors in measurement, I use the increasingly documented connection between international waters and TIP. The inaugural U.S. Department of State (2001) TIP report notes the Hong Kong police force "continuously patrols land and sea boundaries to ensure border integrity and aggressively investigates triad involvement in organized migrant smuggling" (p. 20), and in South Korea's case, much of their transit traffic occurs in their "territorial waters by ship" (p. 97).

The main IV in this paper is hence the log ratio of coastline distance to its land area [both records from The World Factbook (Central Intelligence Agency, 2020)].[13] The assumption is that countries with larger coastlines are at greater risk of trafficking inflows. The ratio of coastline distance to area is preferred over just coastline distance since countries with larger land area naturally have longer coastlines.[14]

[13] `https://github.com/LSYS/country-coastline-distance`.

[14] This approach in no way implies that trafficking only occurs through international waters. In the UNODC [United Nations Office on Drugs and Crimes] (2014) report, information from law enforcement officers in Italy and Spain who specialized in organized crime and human trafficking

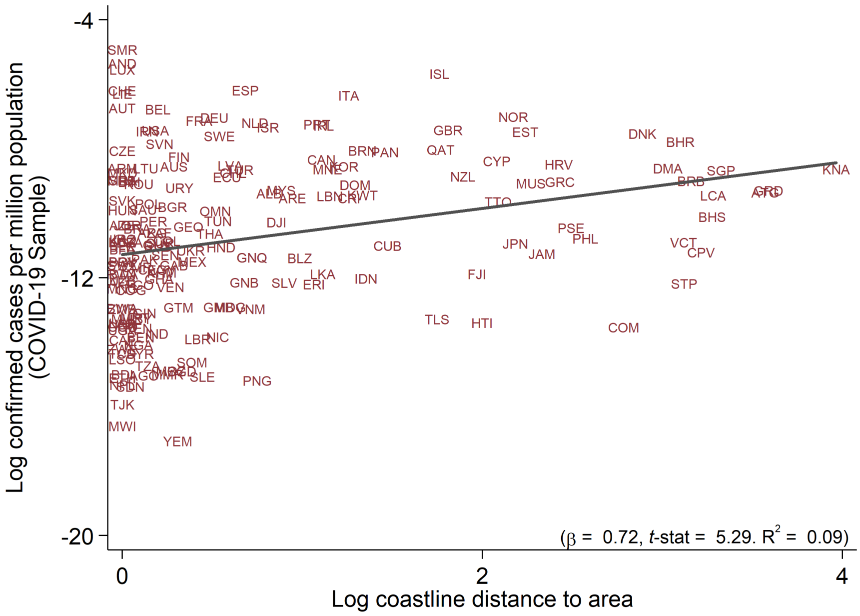

Figure VI: Reduced-Form Relationship: Trafficking and the COVID-19 Pandemic
Notes—Scatterplot of the log confirmed cases per million population by the end of the 3rd month into the COVID-19 pandemic (March 2020), against log coastline distance to area. The highest 5 percentile in log confirmed cases per million population and coastline distance to area omitted in the graph. Estimated β coefficient, its t-statistic, and the R^2 come from a simple linear regression.

A common trafficking route by sea, for example, involves the Mediterranean Sea, with trafficking networks exploiting this route to bring illegal migrants into Europe (U.S. Department of State 2018, p. 407). A large proportion (more than 90 percent) of Mediterranean crossings originate from Libya, a primary departure point for vulnerable migrants from and transiting Libya en route to Europe (U.S. Department of State 2017, p. 432). Spain for instance, have their victims "moved by sea into Southern Spain" (U.S. Department of State 2018, p. 394), and experiences an "increasing number of victims arrived in southern Spain by sea via Morocco" (U.S. Department of State 2019, p. 432).[15]

suggests that trafficking networks utilize existing migration paths by land, sea, and air. "Victims trafficked to Spain, for instance, may fly to the main airports of the country or of neighboring countries. In the case of the land route, they will travel through the Sahel, the Sahara to North Africa and cross the border into Ceuta or Melilla in Spain. Similarly, on the route to Italy, they will attempt the sea passage from North Africa to Lampedusa or Sicily" (UNODC [United Nations Office on Drugs and Crimes] (2014), pp. 56-57).

[15] Another potential channel through which coastline distance can affect the risk of TIP inflow has to do with the former's connection to the fishing industry, which has been increasingly documented in the TIP reports. According to the UNODC [United Nations Office on Drugs and Crimes] (2016) report, trafficking for forced labor in the fishing industry "is commonplace in several parts of the world" (UNODC [United Nations Office on Drugs and Crimes] 2016, p. 8), and is "among the most frequently reported types of forced labour was trafficking in the fishing industry" (UNODC [United Nations Office on Drugs and Crimes] 2016, pp. 103–104). This type of fishing industry trafficking can happen "on board big fishing vessels on the high seas, carried out by large companies that trade fish internationally, or in on-land processing facilities" (UNODC [United Nations Office on Drugs and Crimes] 2016, p. 8). In Singapore for example, a country whose economy has been historically tied to its seaports, fishing captains "engage in forced labor by using physical abuse to force men to perform labor on long-haul boats that transit or dock at Singaporean ports" (U.S. Department of State 2019, p. 418).

Trafficking by sea is also a target of policy. In the fishing industry, one of the recommendations to Ireland is "Amend the atypical working scheme for sea fishers to reduce their risk of labor trafficking" (U.S. Department of State 2019, p. 251). A TIP report recommends that Djibouti trains its Coast Guard to better identify potential trafficking victims transiting by sea (U.S. Department of State 2019, p. 174). In Europe, Finland helped create an anti-trafficking curriculum for "trafficking victim identification for passenger ferry personnel in the Baltic Sea" (U.S. Department of State 2018, p. 188). Italian authorities conducted "joint border patrols and training with Slovenia and Albania, reportedly decreasing trafficking flows across the Adriatic Sea" (U.S. Department of State 2005, p. 131). The Swedish Coast Guard, police, and customs officials participated in similar "joint regional intelligence operations in trafficking cases involving travel by sea" (U.S. Department of State 2019, p. 440). And, in 2015, the United Kingdom passed the *Modern Slavery Act*, applicable to England and Wales, to "provide law enforcement authority to pursue criminals, including human traffickers at sea, and including authority to board, divert, and detain vessels; make arrests; and seize evidence while investigating potential offenses at sea" (U.S. Department of State 2019, p. 412).

Figures V and VI show the reduced-form relationship between the coastline measure and the number of confirmed cases per population for both pandemics. Formally, in the first stage of the two-stage least-squares regression, I treat the relative risk of TIP inflow as endogenous and instrument it with log ratio of countries coastline distance to land area:

$$(\text{Relative TIP inflow})_i = \xi + \pi C_i + \gamma_i + \boldsymbol{X}_i + \nu_i, \tag{3}$$

where C_i is the log of coastline distance to land area. The exclusion restriction is that C_i does not appear in the structural equation (2), or, that conditional on the included controls, the coastline to land area ratio has no direct effect on the modern-day pandemics other than through the opportunities and risks involved in TIP flows.[16]

[16] Another assumption on TIP patterns as implied in the first-stage equation (3) is that the relative TIP inflowfor countries persists through the years, even if annual reported (and actual) figures vary. This is largely because of the lack of data on TIP, and the fact that the annual TIP reports often repeat the order of destination vs. source in their trafficking profiles, so there is little variation across time. Akee et al. (2014) provide theoretical and empirical support for the inelastic demand of trafficked persons, which might explain this persistence, since they find that stricter law enforcement is associated with an increase in the probability of TIP inflow.

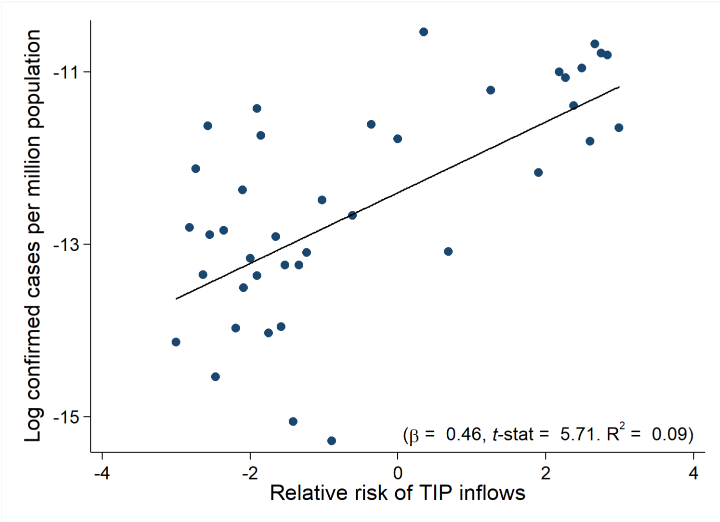

Figure VII: Binned scatterplot of Structural Relationship

Notes—Binned scatterplot of the log confirmed cases per million population by the end of the 3rd month into the H1N1 pandemic (June 2009 for H1N1 and March 2020 for COVID-19), against the relative risk of international trafficking in persons flow measure defined in equation (1). Each bin contains approximately 2.5 percentage of the observations. Estimated β coefficient, its t-statistic, and the R^2 come from a simple linear regression.

Trafficking and Pandemics: OLS Results

Table I report the OLS results from equation (2), regressing log confirmed cases per million population (by 3rd month in the pandemic) on relative TIP inflowmeasure, averaged over 2001–11, where a higher measure indicates a higher risk of being a destination of international TIP. Column (1) includes only the relative TIP inflowmeasure and the COVID-19 dummy, showing the expected direction of risk of TIP inflow on confirmed numbers per population. The COVID-19 dummy is highly significant and large, capturing differences in epidemiological behavior for the H1N1 and COVID-19 pandemics. The R^2 indicates that 48 percent of the variation in pandemic severity is associated with the type of pandemic and relative risk of trafficking inflow to outflow. Figure VII shows the OLS results as a simple linear regression of log confirmed cases per million population against the relative TIP inflowmeasure.[17]

Column (2) includes the 13 region dummies. Column (3) adds four gravity-type controls to the pandemic source (Mexico for H1N1 and China for COVID-19). First is a dummy for whether the country is contiguous to the pandemic source country. Second is a dummy for whether the country shares a common major language with the pandemic source country. Third is the geographical distance to the pandemic source country. The last gravity-type measure is a dummy for whether there is a PTA (preferential trade agreement) with the pandemic source country. These

[17] The implicit assumption with this use of the COVID-19 dummy is that a virus strain has the same epidemiological behavior across countries, conditional on the controls.

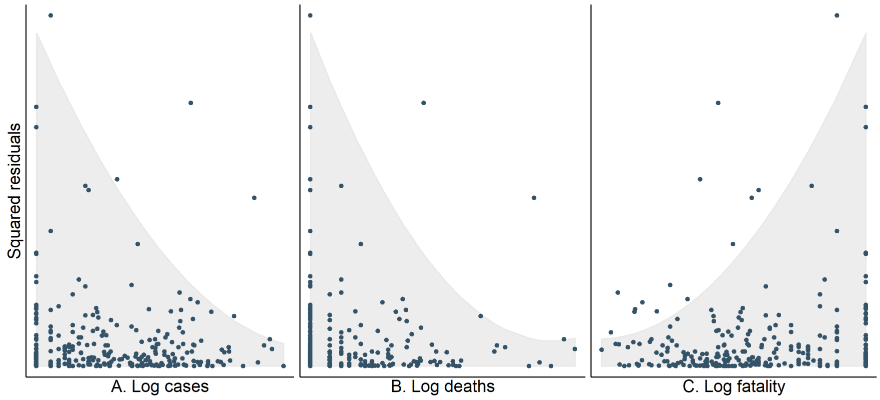

Figure VIII: Scatterplot of OLS Residuals

Notes—Scatterplot of estimated squared residuals from column (3) of Table I, against (A) log confirmed cases, (B) log confirmed deaths, and (C) log of case fatality rate, all by the 3rd month into the pandemics (June 2009 for H1N1 and March 2020 for COVID-19).

controls reduce the OLS estimate only slightly.[18]

WLS and Precision of Estimates. A commonly cited problem with the pandemic reported numbers has to do with the varying precision across countries (e.g. Henriques 2020; Ritchie and Roser 2020). A particular possibility with the behavior of the residuals is that they may be increasing in the reported number of cases, the reported number of deaths, or decreasing in the reported case fatality rate. This creates a measurement error in the dependent variables which decreases precision of standard errors.[19]

With this precision of reported pandemic numbers in mind, I test for the presence of heteroskedasticity specific to the above three measures, both graphically and statistically. Figure VIII shows that the residuals behave in the expected manner, with residuals decreasing in reported cases and deaths, but increasing in case fatality. While the Breusch-Pagan tests of heteroskedasticity for these three measures do not reject the null of constant variance (with ρ-values of 0.45, 0.45, and 0.61), in columns (4)–(6) I weigh the observations by these three measures. The estimates of relative TIP infloware slightly reduced, but the standard errors of relative TIP infloware never lower than the OLS estimate in column (3). Columns (7)–(8) show that the observed results are not driven by a single pandemic episode.

Magnitudes of OLS Estimate. To get a sense of the magnitude and plausibil-

[18] The "economics of language" suggests that sharing a common major language influences the destination of choice among immigrants (Chiswick and Miller 2015), and PTAs might include migration-related provisions that influence migration patterns (Beverelli and Orefice 2019).

[19] An example given is that suppose 100 people are infected, but only 10 become so ill they check in to hospitals. Subsequently, one of the 10 patients die. This gives a case fatality rate of 10% (1/10), when the (true) infection fatality rate is 1% (1/100). Countries with more vigilant testing would both detect more infected individuals and yield a lower fatality estimate. I control for testing numbers in the robustness tests below.

ity of the estimated effect of the relative risk of TIP inflow on pandemic severity, I use the estimate of 0.45 from column (3) of Table I for the comparisons between three European countries with varying estimates of TIP flows—Bulgarian, Bosnia, and Belgium. First, I make a comparison between Bulgaria, which has the relative TIP inflowmeasure of -1.9 (approximately the 25th percentile), indicating that it is more at risk of being a source of trafficking rather than a destination, and Bosnia, which has the relative TIP inflowmeasure of exactly 0 (approximately the 60th percentile), indicating that it is at equal risk of being a source and destination. The estimate of 0.45 for the relative TIP inflowimplies that the difference between the two countries' pandemic severity is 1.35 times ($e^{1.9\times0.45}-1$). In reality, the difference in pandemic severity between these two countries is 0.72 times and 0.77 times for the H1N1 and COVID-19 pandemic, respectively. This is an overestimation of the association between TIP and pandemic severity. On the higher end, I compare in turn Bosnia to Belgium, with a relative TIP inflowmeasure of 2.18 (approximately the 75th percentile). The estimate of 0.45 implies that the difference in pandemic severity is on average 1.66 times. In reality, this difference is 1.54 and 2.25 times for the H1N1 and COVID-19 pandemic, respectively, so the OLS estimate sits between these two ranges.

Summary and Interpretation. The results from Table I overall suggest a substantial but not implausibly large association between the relative risk of TIP inflow and pandemic severity. These estimates however, do not support a causal interpretation. First, as the empirical evidence in the existing literature on human trafficking has consistently shown (Akee et al. 2014; Bales 2007; Cho 2015; Hernandez and Rudolph 2015), flows of human trafficking greatly resembles flows of migration, where more developed countries with better employment opportunities experience higher inflows. These countries are also the ones that are more economically connected, with the busiest air and sea ports, and thus are naturally at higher risk of global disease spread even without considering irregular migrations (e.g. Adda 2016; Oster 2012).

The above introduces bias with a direction that is a priori unpredictable, since countries with better institutions are at higher risk of pandemic severity through economic connectivity, while also being the countries better adapt to respond to it. Finally, the relative TIP inflowmeasure is a broad indicator of TIP and might thus correspond poorly with the true hidden prevalence of international TIP, which biases the OLS estimates downwards. To deal with these concerns, I consider the log of coastline distance to land area as an instrument for countries' relative risk of TIP in the next section.

Trafficking and Pandemics: 2SLS Results

A. Determining the Relative Risk of TIP inflow

Table II documents the proposed channel of log coastline distance to land area increasing the relative risk of TIP inflow. All results are cross-country OLS with the 13 region dummies. Column (1) begins by testing whether anti-TIP standards and victim amnesty predict the relative risk of trafficking inflow. Both work in the expected direction, as has been found in the existing literature (e.g. Cho 2015), with the proposed channel of inelastic demand as the explanation (Akee et al. 2014). In column (2) the polity and constraint on executive scores are not significant, suggesting that broad measures of institutions are not good predictors.

Column (3) includes the proposed main instrument in this paper, the log of coastline distance to land area ratio, with this instrument and the region dummies explaining 31 percent of the variation.[20] Column (4) uses the landlocked and island dummies in place of the coastline to area measure, showing that the proposed channel of international waters increasing the risk of trafficking can also be captured using these alternative geographical measures.

Columns (5)–(7) document the alternative channels of irregular migrant and illegal drug flows that might predict the relative TIP inflow. Column (5) uses historical inflow and outflow ratio of asylum-seekers, averaged over 1990–2005, aggregated up to monadic country level from the UNHCR [United Nations High Commissioner for Refugees] (2019). Flows of trafficked persons and irregular migrants are closely intertwined (Hernandez and Rudolph 2015; Cho 2015). Even with limited data, the UNODC [United Nations Office on Drugs and Crimes] (2016) report suggests that the citizenships of identified trafficking victims are correlated with the citizenships of migrants in the same country and period (pp. 58). The UNODC [United Nations Office on Drugs and Crimes] (2018a) report also notes the relationship between trafficking flows and migrant smuggling flows towards North Africa (pp. 87).

Columns (6)–(7) use the log of cocaine and ATS (amphetamine-type stimulants) drug inflow per capita into countries as predictors of the relative risk of TIP inflow,

[20] Just the region dummies alone explain 22 percent of the variation in relative TIP inflow.

as there are also connections between human and drug trafficking flow patterns. One purpose of TIP itself includes using trafficked persons in drug trafficking operations (UNODC [United Nations Office on Drugs and Crimes] 2014, p. 57). Another connection is in the trafficking routes used, where Nigerian trafficking networks for example "use migrant and drug trafficking routes through Libya and Italy to transport women and girls to France, where they subject them to trafficking" (U.S. Department of State 2019, p.200), and the 2018 *Global Smuggling of Migrants* report states that "There are indications that some groups involved in the smuggling of migrants are also involved in drug trafficking. One of the key routes for cocaine trafficking from South America to Europe passes through West Africa. Along the internal African routes leading to North Africa, both cocaine and migrants may be smuggled to the Mediterranean shores and eventually to Europe" (UNODC [United Nations Office on Drugs and Crimes] 2018b, pp. 53–54). This channel might be explained by how the costs of human trafficking are reduced by tapping on existing smuggling routes of drugs (and also irregular migrants), an association that has been documented in Cho 2015. The drug inflow data in this paper are aggregated up to the destination country from the UNODC [United Nations Office on Drugs and Crimes] (2020b) Individual Drugs Seizure data 2011–16. Drug inflow is also normalized by population size so that bigger countries do not disproportionately affect the estimated results.

The following section presents the two-stage least-squares results using log coastline distance to land area as the main instrument for relative risk in TIP flows, before using alternative instruments in overidentification tests to support the exclusion restriction of the coastline instrument.

B. TIP Inflow and Pandemic Severity

Two-stage least-squares estimates of the structural equation (2) are documented in Table III, with the log of coastline distance to land area as the instrument for relative risk of TIP flows. Panel A reports the 2SLS estimates, and Panel B reports the corresponding first stages. Column (1) shows a highly statistically significant relationship between pandemic severity and the relative TIP inflow measure, with a first-stage heteroskedastic-robust F-statistic of 26, indicating relevance of the instrument. Columns (2)–(4) incrementally add the COVID-19 dummy, the region dummies, and the four gravity controls to the source country of the pandemic. The PTA dummy is negative and significant, suggesting that countries with a preferential trade agreement with the source country of pandemic experience a lower number of cases, which while unexpected, might suggest that these countries are the first ones to formally arrange migration-provisions (Beverelli and Orefice 2019).[21]

Columns (5) and (6) split the sample into the H1N1 and COVID-19 sample, respectively. The estimates suggest that the effect of relative TIP inflowon pandemic severity, by the third month, is larger for the H1N1 sample than the COVID-19 sample, although the estimate for the latter is more precise. The 2SLS estimates are consistently larger than the OLS estimate, and this in theory provides some evidence about the measurement error in the relative TIP inflowmeasure biasing the OLS estimates downwards. In the robustness checks below, I include larger sets of controls which reduces the size of the 2SLS estimates to be closer to, though still larger than, the OLS estimates.

In columns (7)–(8) I run three placebo-type regressions with three measures of fatality as the dependent variable: (i) log of case fatality rate (confirmed deaths divided by confirmed cases), log of crude death rate (confirmed deaths per capita), and (iii) log of (confirmed) deaths, all by the third month into the pandemic. A major concern about the relative TIP inflowmeasure is that it might be highly correlated with institutional factors, since developed countries face more inflows of TIP (Cho 2015; Bales 2007). If this is the case, then we would expect to see that countries with higher risk of trafficking inflows are also those countries with systematically lower fatality rates. Columns (7)–(8) provides some evidence against this concern. Figure IX shows the 2SLS estimates for different months of the pandemic, by the two different pandemic subsamples, and the estimates are similar.

C. Overidentification Tests

Other than placebo tests, another way to test the validity of the coastline instrument is to use overidentification tests using alternative instruments. Here I use trafficking of illegal drugs as the alternative instruments. The exclusion restriction assumption applies in each case—that the consumption and trafficking flows of drugs have no direct effect on pandemic severity other than through their effect on the relative risk of international trafficking flows. In other words, they are rightly excluded from the structural equation (2) of interest. The test statistic for this is the Hansen test statistic, reported in Table IV, for the null hypothesis that the instruments are uncorrelated with the error term in the structural equation (2).

[21] Performing Hausman test using the results from column (4) rejects the null hypothesis that the relative TIP inflowmeasure is exogenous, with $\chi^2 = 19.3$ and a ρ-value < 0.0001, indicating that the OLS results are inconsistent.

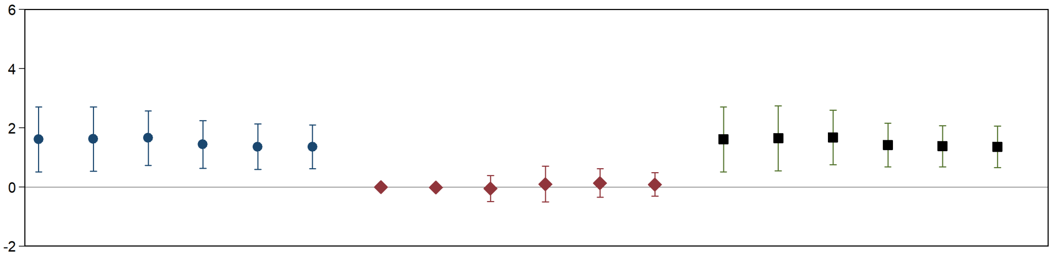

(a) H1N1 Sample

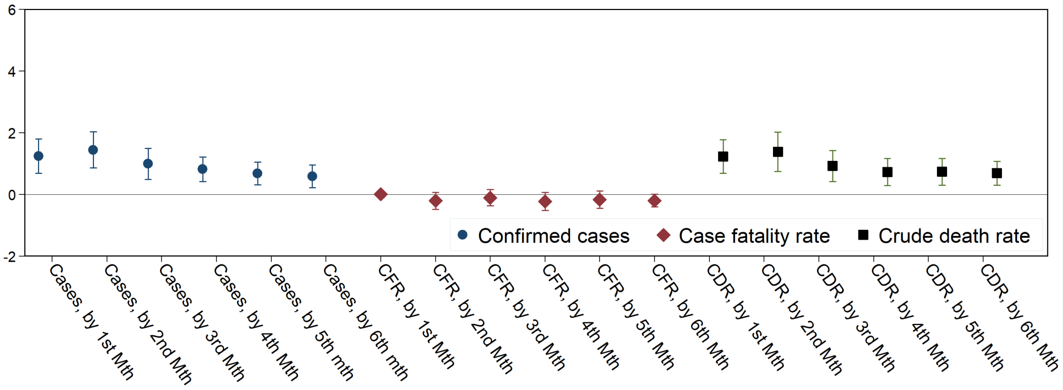

(b) COVID-19 Sample

Figure IX: 2SLS Estimates by Month

Notes—Coefficient plot of two-stage least-squares estimates with the dependent variable as cumulative confirmed numbers by the 1st to 6th month of the pandemic, and by the H1N1 and COVID-19 pandemic subsamples. All regressions control for the 13 region dummies and the gravity controls as in the specifications from Table III. The vertical bars indicate the 95 percent confidence interval constructed using the robust standard errors.

The cocaine seizure data (2012–16) and the drug inflow data (2011–16) come from the Individual Drug Seizures data (UNODC [United Nations Office on Drugs and Crimes] 2020b). I use three instruments from the data: (i) the log of cocaine seizures in a country per capita; (ii) log cocaine inflow per capita; and (iii) log amphetamine (-type stimulants) inflow per capita. A link between drug and human trafficking has to do with both the routes and people involved, with the UNODC [United Nations Office on Drugs and Crimes] (2011) report noting a potential "connection between the smuggling of migrants and the rapidly growing trade in cocaine across the Sahara to North Africa and Europe. In 2005, there were already indications that some migrants were trading small quantities of cocaine over the Sahara" (UNODC [United Nations Office on Drugs and Crimes] 2011, pp.46–47). Smuggler of migrants in the Sahara have also been suspected of "profiting from other forms of illicit trade, notably of cocaine destined ultimately for the European market" (UNODC [United Nations Office on Drugs and Crimes] 2011, p. 63), and in Latin America, there have been reports that migrant smugglers pay "a 'tax' to use routes under the control of drug trafficking organizations" (UNODC [United Nations Office on Drugs and Crimes] 2018b, pp. 98–99).

An advantage of using drug flow and seizure data is that it is almost certainly more comprehensive than numbers of human trafficking, where the "estimated global interception rate of opiates also rose from between 9 and 13 per cent during the period 1980-1997 to between 23 and 32 per cent during the period 2009-2015", and the "estimated global interception rate of cocaine increased to between 45 and 55 per cent in 2015" (UNODC [United Nations Office on Drugs and Crimes] 2017, p.17).

Table IV presents the direct tests of the exclusion restriction on the coastline instrument. The odd-numbered columns use only the alternative instrument for the individual IV estimates, while the even-numbered columns use the main coastline instrument together with the alternative instrument as part of the overidentification test. Panel C presents the alternative version of this test, with the log coastline distance to land area measure included in the structural equation (2)—the second stage—as one of the included regressors. If the coastline instrument is valid, it should not appear as statistically significant here and that is the case. Overall, using drug seizure and trafficking inflow data supports the exclusion restriction of the coastlines instrument, as indicated by the small Hansen test statistics that are all not significant at conventional levels. The next section considers further tests of robustness with specific sets of controls.[22]

Robustness

A. Health and Institutional Factors

In this section, I control for additional variables that could plausibly be correlated with both the relative flow of trafficking and pandemic severity. It turns out that many of the additional controls affect pandemic severity indirectly through the channel of TIP inflow, with their direct effect largely muted in the second stage regressions. Overall, the 2SLS estimates become smaller in magnitude but remain statistically significant.

Table V presents the results with a set of health and institution factors that are plausibly linked to pandemic severity. The results are robust to controls of various

[22] At this point it might be worth noting that using historical asylum-seeker flows (or refugee flows), averaged over 1990–2005, as the instrument also produces similar 2SLS estimates, but fail to pass the overidentification tests when the log coastline distance to area instrument is included. The same happens when using cocaine and amphetamine inflow instruments in place of the coastline instrument. This suggests that broader forms of irregular migration flows have a direct effect on local epidemics, other than through the route connection of trafficked persons.

(a) institutional measures: Anti-TIP standards, amnesty for victims, polity, constraint on executive, and log GDP per capita; (b) government size measures which potentially capture how public officials handle the local epidemics: log government expenditure to GDP, log government health expenditure per capita, log number of tests conducted; and (c) measures of health: old-age dependency (above 64 to working-age population), immunization rates,[23] log infant mortality rate, and the log total health expenditure per capita in the country.[24]

The Anti-TIP and victim amnesty measures are from the Human Trafficking Indicators 2001–11 data (Frank 2013), polity and constraint on executive are from the Polity data (Marshall et al. 2019), the numbers of conducted tests and are from Max Roser, Hannah Ritchie and Hasell (2020), and all other measures are from the World Development Indicators World Bank (2019). Column (9) includes all the additional controls together except for the log conducted test numbers, which is available only for the COVID-19 sample.

Two observations might be worth noting here. First, the number of tests conducted is not correlated to the confirmed numbers, providing evidence that observed differences in reported numbers across countries are not just an artifact of testing policies (column (5)). The standard error however, is substantially smaller (in fact, the smallest).

Second, the 2SLS estimate of relative TIP inflowtends to be smaller than the baseline 2SLS estimates in Table III, but remains statistically significant except for in column (8) with the log health expenditure per capita measure, which is highly correlated with the relative TIP inflowmeasure in the first stage. The first-stage becomes very weak as a result of the inclusion of the log health expenditure per capita measure, with a F-statistic of 3.0, leading to an insignificant second-stage estimate. Hence I turn to the Anderson-Rubin Wald test as an alternative diagnostic test that is robust to a weak first stage. The χ^2-test statistic of 40.8 and ρ-value < 0.0001, rejects the null that the relative TIP inflowmeasure is statistically equal to zero, indicating that the expected association between relative TIP inflowand pandemic numbers is still present despite the weak first stage. Nonetheless, I take this as another indication that caution is needed with interpretation of the results. Overall, the 2SLS measure is robust to controlling institutional and

[23] Immunization rates are averages for DPT (diphtheria, pertussis, and tetanus), Hepatitis B 3rd dose, and Measles

[24] Using average expropriation risk instead of the constrain on executive or polity measure gives similar results.

health measures, and least robust with log health expenditure per capita.[25]

B. Social and Cultural Factors

Table VI considers social and cultural factors, such as the size of government welfare in column (1), which is not significant. Column (2) controls for school enrollment rate, and countries with higher secondary school enrollment have higher confirmed cases per population, which might be because schools are places with one of the largest gatherings of people.[26]

Controls for other potential sources of mass congregation that potentially increase spread (e.g. Rocklöv and Sjödin 2020) include the percentage of Protestant, Muslim, and Roman Catholic in a country, the level of ethno-linguistic fragmentation (both from La Porta et al. 1999),[27] and a dummy for whether there are mass mobilization and protests within the first four months of the pandemic, which are constructed from Mass Mobilization Data Project (Clark and Regan 2016). Columns (6) and (7) control for population density and urbanization that might affect the spread of infectious diseases, and column (8) controls for total fisheries production since dependence on production at sea might be correlated with both institution measures and the coastline instrument. Column (9) includes all the variables except for the mass mobilization and protests, which is available only for the H1N1 sample. The 2SLS estimate remains significant, with a smaller estimate of 0.56.

C. Cross-country Movement Factors

Table VII presents the 2SLS results with an additional set of controls for migration and tourism. The migration flow data are from Abel and Cohen (2019), which contains 5-year bilateral international migration flow average estimates. Refugee and asylum-seeker flows come from the UNHCR [United Nations High Commissioner for Refugees] (2019), and the tourism and refugee stock data comes from the World Bank (2019).

In column (1), it turns out that migration inflow from the pandemic source country is not positively correlated with the local epidemic spread. Similarly, once the

[25] Using the cocaine seizures and inflow data as the instrument does not have the same weak first stage problem, and the 2SLS estimate is similar to the baseline and significant at the 5% level (untabulated).

[26] The primary school enrollment variable is not significant, and this might be because primary school enrollment has much lower variation across countries—secondary enrollment has more than twice the standard deviation of primary enrollment in the data.

[27] Ethno-linguistic fragmentation has been linked to both trafficking flows (Akee et al. 2010) and economic growth (Easterly and Levine 1997).

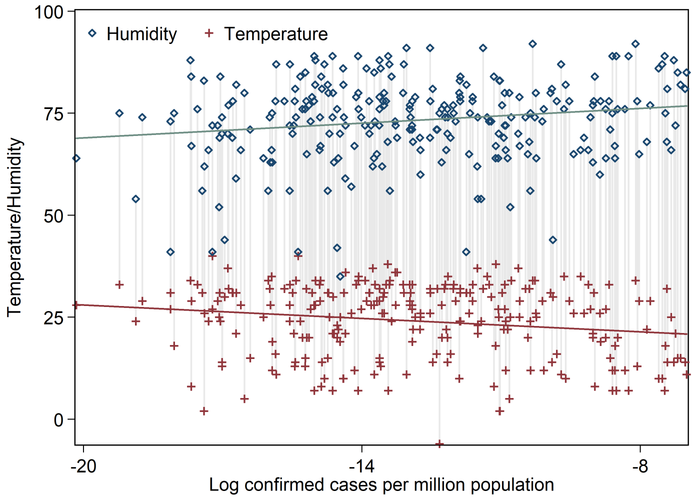

Figure X: Temperature and Humidity Effects on Confirmed Numbers

Notes—Scatterplot and linear fit of temperature and humidity on the log confirmed cases per million population, by the end of the 3rd month into the H1N1 pandemic (June 2009 for H1N1 and March 2020 for COVID-19). Temperature is the minimum monthly high (degree Celsius) and (relative) humidity is the afternoon maximum, both measures are taken directly from Acemoglu et al. (2001), originally from Parker (1997).

risk of TIP inflow is controlled for, the inflow of both regular and irregular migrants does not increase the local numbers. The stock of migrants and refugees in a country likewise does not increase local numbers. The tourism receipts as a percentage of total exports however, is positive and statistically significant in column (8). Overall, the 2SLS estimate drops to a more conservative 0.74 in column (9) where all controls are included at once. The flows and stock of migrants do not appear to be correlated with the local numbers in the expected (positive) manner, although countries with a larger dependence on tourism in their export sector face consistently higher local confirmed cases per population.

D. Geographical Factors

The final set of controls I consider are geographical factors which are potentially correlated with both risk of trafficking inflows and other economic-related factors (e.g. Bloom and Sachs 1998; Gallup et al. 1999; Dell et al. 2012; Nunn and Puga 2012), presented in Table VIII. In column (2), the (absolute) latitude variable is positive and significant at the 10 percent level, consistent with studies finding that the hotter climates in countries further away from the equator impedes the spread of local epidemics (Bloom-Feshbach et al. 2013; Ma et al. 2020; Wang et al. 2020). This is further confirmed in column (4), where countries with higher mean temperatures have consistently lower confirmed numbers. Figure X show this relationship diagrammatically, which also shows that the humidity measure is positively associated with confirmed cases. In columns (5)–(7), I further control for a set of temperature, humidity, and soil quality/climate variables and report the ρ-value in brackets for their joint test of significance.

Overall, the geographical factors mostly work in the expected direction, with higher temperatures associated with lower confirmed numbers, and the 2SLS estimate of relative TIP inflowagain drops to a more conservative value, 0.81, with higher precision when all the geography controls are included in column (8).[28]

E. Placebo Tests for Coastline Instrument

Finally, Table IX provides a set of falsification tests. Using migration inflow and refugee inflow as the instruments do not lead to a detectable effect of TIP inflow, suggesting that the coastline porosity measure is not just capturing broader patterns of irregular migration. The GDP measure shows that the main 2SLS results are not just capturing the wealth of countries, which is a primary concern since irregular migration tends to flow from poorer to richer countries. I also consider urbanization, since countries with relatively smaller areas (larger coastline to area) have higher urbanization, which potentially drives epidemic spread. It turns out that the measure of urbanization is significant in the second stage, but does not invalidate the main 2SLS results to the extent that the first-stage and reduced forms are significant but with the wrong signs—urbanization is negatively correlated with TIP inflow and case numbers. The remaining alternate instruments mitigate concerns that the coastline instrument inadvertently captures other factors that might be correlated with pandemic severity: the size of the tourism industry, size of the fishery industry (as a coast-related informal sector), and the stock of refugees.

Concluding Remarks

Many of the studies on the spread of epidemics and pandemics look at the travel restrictions and movement of people as a factor. Hence, there is consensus that mobility—international and local—has an effect on disease spread. This paper specifically examines the link between trafficking and pandemic severity, suggesting that countries with higher indicated trafficking inflow have more cases per population.

[28] One caveat is that the estimates become considerably noisier when (Northern and Western) European countries are excluded from the sample (Figure A2), suggesting that these countries disproportionately influence the results.

Even if the evidence is interpreted as descriptive, the safety and living conditions of irregular migrants during a pandemic should not be overlooked. Futhermore, identifying which places are vulnerable during a pandemic remains a first-order challenge, and the analyses show systematic rather than idiosyncratic cross-country differences.

I end with two caveats. First, the implication is not that trafficked persons cause epidemics per se. Rather, illegal migrants bypass medical screenings and potentially become part of the community who are positive but undocumented. Based on the epidemiology literature, such undocumented cases account for the vast majority of infections. Second is the issue of measurement, with TIP inflow constructed from indicators rather than actual numbers (as is the case with all comprehensive studies on TIP). Better data on trafficking is needed to improve our understanding of the trafficking–epidemic connection.

References

Abel, G. J. and J. E. Cohen (2019). Bilateral International Migration Flow Estimates for 200 Countries. *Scientific Data 6*(1), 82.

Acemoglu, D., S. Johnson, and J. A. Robinson (2001). The Colonial Origins of Comparative Development: An Empirical Investigation. *American Economic Review* (5), 1369.

Adda, J. (2016). Economic Activity and the Spread of Viral Diseases: Evidence from High Frequency Data. *The Quarterly Journal of Economics 131*(2), 891–941.

Agence France-Presse [AFP] (2020). Why Italy? the Factors behind a Coronavirus Disaster.

Akee, R., A. K. Basu, A. Bedi, and N. H. Chau (2014). Transnational Trafficking, Law Enforcement, and Victim Protection: A Middleman Trafficker's Perspective. *The Journal of Law and Economics 57*(2), 349–386.

Akee, R., A. K. Basu, N. H. Chau, and M. Khamis (2010). Chapter 28 Ethnic Fragmentation, Conflict, Displaced Persons and Human Trafficking: An Empirical Analysis. In G. S. Epstein and I. N. Gang (Eds.), *Migration and Culture*, Volume 8 of *Frontiers of Economics and Globalization*, pp. 691–716. Emerald Group Publishing Limited.

Bales, K. (2007). What Predicts Human Trafficking? *International Journal of Comparative and Applied Criminal Justice 31*(2), 269–279.

Beverelli, C. and G. Orefice (2019). Migration Deflection: The Role of Preferential Trade Agreements. *Regional Science and Urban Economics 79*, 103469.

Bloom, D. E. and J. D. Sachs (1998). Geography, Demography, and Economic Growth in Africa. *Brookings Papers on Economic Activity*, 207–73.

Bloom-Feshbach, K., W. J. Alonso, V. Charu, J. Tamerius, L. Simonsen, M. A. Miller, and C. Viboud (2013). Latitudinal Variations in Seasonal Activity of Influenza and Respiratory Syncytial Virus (Rsv): A Global Comparative Review. *PloS one 8*(2), e54445–e54445.

Bogoch, I. I., O. J. Brady, M. U. G. Kraemer, M. German, M. I. Creatore, M. A. Kulkarni, J. S. Brownstein, S. R. Mekaru, S. I. Hay, E. Groot, A. Watts, and K. Khan (2016). Anticipating the International Spread of Zika Virus from Brazil. *The Lancet 387*(10016), 335–336.

Central Intelligence Agency (2020). CIA World Factbook.

Chinazzi, M., J. T. Davis, M. Ajelli, C. Gioannini, M. Litvinova, S. Merler, A. Pastore y Piontti, K. Mu, L. Rossi, K. Sun, C. Viboud, X. Xiong, H. Yu, M. E. Halloran, I. M. Longini, and A. Vespignani (2020). The Effect of Travel Restrictions on the Spread of the 2019 Novel Coronavirus (Covid-19) Outbreak. *Science 368*(6489), 395 LP – 400.

Chiswick, B. R. and P. W. Miller (2015). Chapter 5 - International Migration and the Economics of Language. In B. R. Chiswick and P. W. Miller (Eds.), *Handbook of the Economics of International Migration*, Volume 1, pp. 211–269. North-Holland.

Cho, S.-Y. (2015). Modeling for Determinants of Human Trafficking: An Empirical Analysis. *Social Inclusion 3*(1).

Cho, S.-Y., A. Dreher, and E. Neumayer (2013). Does Legalized Prostitution Increase Human Trafficking? *World Development 41*, 67–82.

Clark, D. and P. Regan (2016). Mass Mobilization Protest Data. *Harvard Dataverse*.

CTDC (Counter-Trafficking Data Collaborative) (2017). Counter Trafficking Data Collaborative Data Codebook.

Dell, M., B. F. Jones, and B. A. Olken (2012). Temperature Shocks and Economic Growth: Evidence from the Last Half Century. *American Economic Journal: Macroeconomics 4*(3), 66–95.

Easterly, W. and R. Levine (1997). Africa's Growth Tragedy: Policies and Ethnic Divisions. *The Quarterly Journal of Economics 112*(4), 1203–1250.

Fang, H., L. Wang, and Y. Yang (2020). Human Mobility Restrictions and the Spread of the Novel Coronavirus (2019-nCoV) in China. *NBER Working Paper No. 26906*.

Ferguson, N. M., D. A. T. Cummings, C. Fraser, J. C. Cajka, P. C. Cooley, and D. S. Burke (2006). Strategies for Mitigating an Influenza Pandemic. *Nature 442*(7101), 448–452.

Frank, R. W. (2013). Human Trafficking Indicators, 2000-2011: A New Dataset. *Harvard Dataverse, V1*.

Gallup, J. L., J. D. Sachs, and A. D. Mellinger (1999). Geography and Economic Development. *International Regional Science Review 22*(2), 179–232.

Gathmann, C. (2008). Effects of Enforcement on Illegal Markets: Evidence from Migrant Smuggling along the Southwestern Border. *Journal of Public Economics 92*(10), 1926–1941.

Greenaway, C. and B. D. Gushulak (2017). Chapter 16: Pandemics, Migration and Global Health Security. In P. Bourbeau (Ed.), *Handbook on Migration and Security*, pp. 316–336. Cheltenham, UK: Edward Elgar Pub.

Gurevich, T. and P. Herman (2018). The Dynamic Gravity Dataset: 1948-2016. *Working Paper 2018-02-A*.

Henriques, M. (2020). Coronavirus: Why Death and Mortality Rates Differ. *BBC*.

Hernandez, D. and A. Rudolph (2015). Modern Day Slavery: What Drives Human Trafficking in Europe? *European Journal of Political Economy 38*, 118–139.

Jakobsson, N. and A. Kotsadam (2013). The Law and Economics of International Sex Slavery: Prostitution Laws and Trafficking for Sexual Exploitation. *European Journal of Law and Economics 35*(1), 87–107.

Khan, K., R. Eckhardt, J. S. Brownstein, R. Naqvi, W. Hu, D. Kossowsky, D. Scales, J. Arino, M. MacDonald, J. Wang, J. Sears, and M. S. Cetron (2013). Entry and Exit Screening of Airline Travellers during the a(h1n1) 2009 Pandemic: A Retrospective Evaluation. *Bulletin of the World Health Organization 91*(5), 368–376.

Kraemer, M. U. G., C.-H. Yang, B. Gutierrez, C.-H. Wu, B. Klein, D. M. Pigott, L. du Plessis, N. R. Faria, R. Li, W. P. Hanage, J. S. Brownstein, M. Layan, A. Vespignani, H. Tian, C. Dye, O. G. Pybus, and S. V. Scarpino (2020, may). The Effect of Human Mobility and Control Measures on the COVID-19 Epidemic in China. *Science 368*(6490), 493 LP – 497.

Kuchler, T., D. Russel, and J. Stroebel (2020). The Geographic Spread of COVID-19 Correlates with Structure of Social Networks as Measured by Facebook. *CESifo Working Paper No. 8241*.

La Porta, R., F. Lopez-de Silanes, A. Shleifer, and R. Vishny (1999). The Quality of Government. *Journal of Law, Economics, and Organization 15*(1), 222–279.

Li, R., S. Pei, B. Chen, Y. Song, T. Zhang, W. Yang, and J. Shaman (2020). Substantial Undocumented Infection Facilitates the Rapid Dissemination of Novel Coronavirus (Sars-Cov-2). *Science 368*(6490), 489 LP – 493.

Long, Y.-s., Z.-m. Zhai, L.-l. Han, J. Kang, Y.-l. Li, Z.-h. Lin, L. Zeng, D.-y. Wu, C.-q. Hao, M. Tang, Z. Liu, and Y.-c. Lai (2020). Quantitative Assessment of the Role of Undocumented Infection in the 2019 Novel Coronavirus (Covid-19) Pandemic. *arXiv*, 1–29.

Ma, Y., Y. Zhao, J. Liu, X. He, B. Wang, S. Fu, J. Yan, J. Niu, J. Zhou, and B. Luo (2020). Effects of Temperature Variation and Humidity on the Death of COVID-19 in Wuhan, China. *Science of The Total Environment 724*, 138226.

Marshall, M. G., T. R. Gurr, and K. Jaggers (2019). Polity IV Project. *Polity IV Project*, 1–86.

Max Roser, Hannah Ritchie, E. O.-O. and J. Hasell (2020). Coronavirus Pandemic (COVID-19). *Our World in Data*.

Nunn, N. and D. Puga (2012). Ruggedness: The Blessing of Bad Geography in Africa. *Review of Economics and Statistics 94*(1), 20–36.

Oster, E. (2012). Routes of Infection: Exports and HIV Incidence in Sub-saharan Africa. *Journal of the European Economic Association 10*(5), 1025–1058.

Page, K. R., M. Venkataramani, C. Beyrer, and S. Polk (2020). Undocumented U.S. Immigrants and Covid-19. *New England Journal of Medicine*.

Parker, P. M. (1997). *National Cultures of the World: A Statistical Reference, Cross-Cultural Statistical Encyclopedia of the World* (4 ed.). Westport, CT: Greenwood Press.

Ritchie, H. and M. Roser (2020). What Do We Know about the Risk of Dying from COVID-19? *Our World in Data*.

Rocklöv, J. and H. Sjödin (2020). High Population Densities Catalyse the Spread of COVID-19. *Journal of Travel Medicine*.

Simon, M. (2020). Why the Coronavirus Hit Italy So Hard.

Slack, J. and H. Campbell (2016). On Narco-coyotaje: Illicit Regimes and Their Impacts on the US–Mexico Border. *Antipode 48*(5), 1380–1399.

Spener, D. (2004). Mexican Migrant-Smuggling: A Cross-Border Cottage Industry. *Journal of International Migration and Integration / Revue de l'integration et de la migration internationale 5*(3), 295–320.

St John, R. K., A. King, D. de Jong, M. Bodie-Collins, S. G. Squires, and T. W. S. Tam (2005). Border Screening for SARS. *Emerging infectious diseases 11*(1), 6–10.

UNHCR [United Nations High Commissioner for Refugees] (2019). Population Statistics. *Vienna: UNODC*.

UNODC [United Nations Office on Drugs and Crimes] (2011). The Role of Organized Crime in the Smuggling of Migrants from West Africa to the European Union. *Vienna: UNODC*.

UNODC [United Nations Office on Drugs and Crimes] (2014). Global Reporton Trafficking in Persons. *Vienna: UNODC*.

UNODC [United Nations Office on Drugs and Crimes] (2016). Global Reporton Trafficking in Persons. *Vienna: UNODC*.

UNODC [United Nations Office on Drugs and Crimes] (2017). World Drug Report. *Vienna: UNODC*.

UNODC [United Nations Office on Drugs and Crimes] (2018a). Global Reporton Trafficking in Persons. *Vienna: UNODC*.

UNODC [United Nations Office on Drugs and Crimes] (2018b). Global Study on Smuggling of Migrants. *Vienna: UNODC*.

UNODC [United Nations Office on Drugs and Crimes] (2020a). How COVID-19 Restrictions and the Economic Consequences Are Likely to Impact Migrant Smuggling and Cross-Border Trafficking in Persons to Europe and North America. *Vienna: UNODC*.

UNODC [United Nations Office on Drugs and Crimes] (2020b). Individual Drug Seizure Cases (IDS). *DATAUNODC*.

U.S. Department of State (2001). Trafficking in Persons Report. *Washington, D.C.: U.S. Department of State.*.

U.S. Department of State (2005). Trafficking in Persons Report. *Washington, D.C.: U.S. Department of State.*.

U.S. Department of State (2009). Trafficking in Persons Report. *Washington, D.C.: U.S. Department of State.*.

U.S. Department of State (2017). Trafficking in Persons Report. *Washington, D.C.: U.S. Department of State.*.

U.S. Department of State (2018). Trafficking in Persons Report. *Washington, D.C.: U.S. Department of State.*.

U.S. Department of State (2019). Trafficking in Persons Report. *Washington, D.C.: U.S. Department of State.*.

Wang, M., A. Jiang, L. Gong, L. Luo, W. Guo, C. Li, J. Zheng, C. Li, B. Yang, J. Zeng, Y. Chen, K. Zheng, and H. Li (2020). Temperature Significant Change COVID-19 Transmission in 429 Cities. *medRxiv*, 2020.02.22.20025791.

Wickramage, K., L. O. Gostin, E. Friedman, P. Prakongsai, R. Suphanchaimat, C. Hui, P. Duigan, E. Barragan, and D. R. Harper (2018). Missing: Where Are the Migrants in Pandemic Influenza Preparedness Plans? *Health and human rights 20*(1), 251–258.

Williams, H. A., R. L. Dunville, S. I. Gerber, D. D. Erdman, N. Pesik, D. Kuhar, K. A. Mason, L. Haynes, L. Rotz, J. St Pierre, S. Poser, S. Bunga, M. A. Pallansch, D. L. Swerdlow, and M.-C. W. Group (2015). CDC's Early Response to a Novel Viral Disease, Middle East Respiratory Syndrome Coronavirus (MERS-CoV), September 2012-May 2014. *Public health reports (Washington, D.C. : 1974) 130*(4), 307–317.

World Bank (2019). World Development Indicators.

Tables

Table I—*OLS Regressions*

	Full Sample (1)	Full Sample (2)	Full Sample (3)	Full Sample (4)	Full Sample (5)	Full Sample (6)	H1N1 Sample (7)	COVID-19 Sample (8)
	Dependent variable is Log confirmed cases, by 3rd month							
Relative TIP inflow	0.53^{***}	0.46^{***}	0.45^{***}	0.41^{***}	0.41^{***}	0.46^{***}	0.46^{***}	0.39^{***}
	(0.06)	(0.06)	(0.05)	(0.07)	(0.07)	(0.06)	(0.07)	(0.08)
Covid-19 dummy	4.06^{***}	4.43^{***}	4.09^{***}	4.58^{***}	4.72^{***}	4.47^{***}		
	(0.27)	(0.23)	(0.28)	(0.39)	(0.30)	(0.35)		
Contiguity dummy			-1.21^{*}	-1.20^{**}	-0.97	-1.49^{***}	-0.86	-2.34^{***}
			(0.63)	(0.59)	(0.61)	(0.54)	(0.63)	(0.84)
Common lang. dummy			1.05^{*}	1.30	1.34	0.59	0.23	2.21^{*}
			(0.57)	(0.80)	(0.88)	(0.65)	(0.46)	(1.18)
Distance from Gzero			-0.08^{**}	-0.08	-0.06	-0.12^{***}	0.16	-0.06
			(0.04)	(0.05)	(0.04)	(0.04)	(0.11)	(0.13)
PTA dummy			-0.92^{***}	-0.46	-0.41	-0.48	-0.82^{**}	1.72^{***}
			(0.34)	(0.52)	(0.44)	(0.53)	(0.39)	(0.53)
Region dummies		Yes	Yes	Yes	Yes	Yes	Yes	Yes
F-test: Regions=0		14.87^{***}	12.86^{***}	16.39^{***}	16.68^{***}	14.5^{***}	23.05^{***}	22.46^{***}
F-test: Gravity=0			4.14^{**}	2.5^{**}	2.4^{**}	3.57^{**}	1.96	8.59^{***}
R^2	0.48	0.66	0.68	0.68	0.73	0.70	0.56	0.65
Weighted by				Cases	Deaths	Fatality		
Countries	172	172	172	172	172	172	134	167
Observations	301	301	301	301	301	300	134	167

Notes—Dependent variable is the log of confirmed cases of the diseases, per million population, by the 3rd month into the pandemics (June 2009, and March 2020, for the H1N1 and COVID-19 pandemics, respectively). The relative TIP inflowmeasure is the ratio of whether a country is reported as mainly a destination or source in international trafficking in persons (TIP), averaged over the years 2001–11, which the annual indicators taken directly from Frank (2013), originally from the annual U.S. Department of State (2001) TIP reports, where a higher score means higher risk of being a destination for TIP. The gravity-type controls come from Gurevich and Herman (2018), for the years 2008 and 2016 (latest available) for the H1N1 and COVID-19 pandemic, respectively. The 13 region dummies are: Africa, Carribbean, Central America, Central Asia, East Asia, Eurasia, Europe, Middle East, North America, Pacific, South America, South Asia, and Southeast Asia. Columns (4)–(6) are weighted-least squares regressions where observations are weighted by: log confirmed cases, log deaths, and the (inverse) log case fatality rate, respectively. Robust standard errors in parentheses.

*** Significant at the 1 per cent level.

** Significant at the 5 per cent level.

* Significant at the 10 per cent level.

Table II—*Predicting Relative Risk of International TIP inflow*

	(1)	(2)	(3)	(4)	(5)	(6)	(7)
	Dependent variable is *relative TIP inflow*						
Anti-TIP standards	2.28***						
	(0.52)						
TIP victims amnesty	2.58***						
	(0.60)						
Polity measure of democracy		−0.01					
		(0.12)					
Constraint on Executive		−0.17					
		(0.37)					
Log coastline to area			0.54***				
			(0.17)				
Island dummy				0.90**			
				(0.45)			
Landlock dummy				−0.99***			
				(0.35)			
Log asylum-seeker flow ratio					0.25***		
					(0.03)		
Log cocaine inflow per capita						0.29***	
						(0.06)	
Log amphetamine inflow per capita							0.32***
							(0.08)
Region dummies	Yes	Yes	Yes	Yes	Yes	Yes	Yes
R^2	0.40	0.59	0.31	0.30	0.41	0.34	0.32
Countries	172	109	172	172	172	172	172
Observations	172	109	172	172	172	172	172

Notes—The dependent variable is the relative risk of international TIP (trafficking in persons) inflow, defined in equation (1). Anti-TIP standards is the minimum standards indicator from Frank (2013), coded 1 in a given year if the TIP report states that the country fully complies with minimum standards for elimination of trafficking. TIP victim amnesty is the victim protective services from the same data. Both are averaged over the years 2001–11. The polity and constraint on executive measures are averaged over 2000-18, from the Marshall et al. (2019) Polity data. Log of coastline distance to land area measures come from the World Factbook Central Intelligence Agency (2020). Log asylum-seekers flow ratio is the ratio of historical inflow to outflow of asylum-seekers, for the years 1990–2005, with data from UNHCR [United Nations High Commissioner for Refugees] (2019). Drug inflow data (kg), are taken from the UN's individual drug seizure cases UNODC [United Nations Office on Drugs and Crimes] (2020b), averaged over the available years of 2011–16. All regressions are OLS and include the 13 region dummies. Robust standard errors in parentheses.

*** Significant at the 1 per cent level.

** Significant at the 5 per cent level.

* Significant at the 10 per cent level.

Table III—*2SLS Regressions of Confirmed Cases (by 3rd Month)*

	(1)	(2)	(3)	(4)	(5)	(6)	(7)	(8)	(9)
							Placebo regressions		
							Dep. var. are log of		
	Dep. var. is Log confirmed cases (per million population)						CFR	CDR	Deaths
	Panel A: Two-Stage Least Squares								
Relative TIP inflow	1.10***	1.46***	1.47***	1.46***	1.66***	0.99***	−0.11	1.35***	−0.11
	(0.24)	(0.28)	(0.31)	(0.30)	(0.48)	(0.25)	(0.12)	(0.30)	(0.08)
Covid-19 dummy		4.43***	4.59***	3.93***			−2.79***	1.57**	−0.84***
		(0.37)	(0.32)	(0.38)			(0.14)	(0.65)	(0.26)
Contiguity dummy				0.17	−1.90*	−0.92	0.30	0.36	−0.21
				(0.81)	(1.05)	(0.95)	(0.45)	(0.70)	(0.27)
Common language dummy				0.47	0.62	1.35	−1.01***	−0.46	−0.63***
				(0.73)	(1.22)	(1.26)	(0.34)	(0.77)	(0.24)
Distance from Gzero				−0.10*	0.24	−0.27	0.02	−0.08	0.01
				(0.05)	(0.22)	(0.16)	(0.02)	(0.05)	(0.02)
PTA dummy				−1.29***	−1.31*	1.66**	−0.81***	−2.03***	−0.51***
				(0.48)	(0.72)	(0.66)	(0.18)	(0.47)	(0.15)
Log confirmed cases								−0.09	0.60***
								(0.12)	(0.05)
First-stage F-stat	26.00	24.62	21.74	23.55	7.31	23.79	23.55	24.25	24.25
	Panel B: First Stage for *relative TIP inflow*								
Log coastline to area	0.60***	0.59***	0.61***	0.61***	0.55***	0.70***	0.61***	0.32**	0.62***
	(0.12)	(0.12)	(0.13)	(0.13)	(0.20)	(0.14)	(0.13)	(0.14)	(0.12)
	Panel C: Ordinary Least Squares								
Relative TIP flow	0.44***	0.53***	0.45***	0.45***	0.45***	0.39***	−0.08**	0.04	−0.00
	(0.08)	(0.06)	(0.06)	(0.05)	(0.07)	(0.08)	(0.04)	(0.04)	(0.03)
Region dummies			Yes	Yes	Yes	Yes	Yes	Yes	Yes
Gravity controls				Yes	Yes	Yes	Yes	Yes	Yes
Countries	172	172	172	172	134	167	172	172	172
Observations	301	301	301	301	134	167	301	301	301

Notes—The dependent variable in columns (1)–(6) is the log confirmed cases of the diseases, per million population, by the 3rd month into the pandemics. In columns (7)–(9) the dependent variables are log of case fatality rate (CFR), number of confirmed deaths divided by number of confirmed cases; log of crude death rate, number of confirmed deaths divided by population, and log confirmed number of deaths. Panel A reports the two-stage least-squares estimates, with the log coastline distance to land area as the instrument for *relative TIP inflow*. Panel B reports the corresponding first stages; Panel C reports the analogous OLS estimates. Columns (3)–(9) include the 13 region dummies. Columns (4)–(9) includes the four gravity-type controls. All panels include the same set of covariates, but are not always reported in Panels B, C, and D to conserve on space. Robust standard errors in parentheses.

*** Significant at the 1 per cent level.

** Significant at the 5 per cent level.

* Significant at the 10 per cent level.

Table IV—*Overidentification Tests*

	(1)	(2)	(3)	(4)	(5)	(6)
	Panel A: Two-Stage Least Squares					
Relative TIP inflow	1.06***	1.05***	1.19***	1.30***	1.62***	1.55***
	(0.27)	(0.21)	(0.29)	(0.23)	(0.37)	(0.29)
First-stage F-stat	82.52	60.50	50.19	34.90	31.87	20.64
Hansen test		.02		.6		.16
	Panel B: First Stage for *relative TIP inflow*					
Log cocaine seizures per capita	0.35***	0.31***				
	(0.04)	(0.04)				
Log cocaine inflow per capita			0.32***	0.28***		
			(0.05)	(0.04)		
Log amphetamine inflow per capita					0.34***	0.25***
					(0.06)	(0.07)
Log coastline to area		0.64***		0.49***		0.39***
		(0.14)		(0.13)		(0.14)
	Panel C: Log of Coastline distance to land area as exogenous in second stage					
Relative TIP flow		1.07***		1.13***		1.75***
		(0.31)		(0.33)		(0.64)
Log coastline to area		−0.04		0.20		−0.17
		(0.30)		(0.25)		(0.45)
Region dummies	Yes	Yes	Yes	Yes	Yes	Yes
Gravity controls	Yes	Yes	Yes	Yes	Yes	Yes
Countries	131	131	172	172	172	172
Observations	242	242	301	301	301	301

Notes—Panel A reports the two-stage least-squares results where the dependent variable is the log of confirmed cases of the diseases, per million population, by the 3rd month into the pandemics; Panel B reports the corresponding first stages; Panel C reports the second stage results with the alternative instruments as the only instrument for *relative TIP flow*, and with log coastline distance to land area entered as an exogenous (included instrument) in the second stage. All regressions include the 13 region dummies, the COVID-19 dummy, and the gravity-type controls from Table III. All panels include the same set of covariates, but are not always reported in Panels B and C to conserve on space. Cocaine seizure (2012–16) and the drugs inflow data (2006–11) are from UNODC [United Nations Office on Drugs and Crimes] (2020b). Robust standard errors in parentheses.

*** Significant at the 1 per cent level.

** Significant at the 5 per cent level.

* Significant at the 10 per cent level.

Table V—*Institutional and Health Factors*

	(1)	(2)	(3)	(4)	(5)	(6)	(7)	(8)	(9)
	Panel A: Two-Stage Least Squares								
Relative TIP inflow	1.53***	1.06***	2.47**	1.73**	0.61***	1.41***	1.88**	2.69*	0.71**
	(0.28)	(0.24)	(1.21)	(0.75)	(0.15)	(0.32)	(0.75)	(1.59)	(0.33)
Anti-TIP standards	−1.65**								−0.58
	(0.79)								(0.48)
TIP victims amnesty	−3.17***								−0.81
	(1.02)								(0.62)
Polity measure of democracy		−0.03							−0.06
		(0.09)							(0.06)
Constraint on executive		0.23							0.26
		(0.26)							(0.21)
Log GDP per capita			−2.39						0.11
			(1.72)						(0.40)
Log government expenditure of GDP				0.01					−0.05
				(0.05)					(0.04)
Log government health expenditure per capita				−0.88					0.02
				(0.75)					(0.33)
Log conducted tests (COVID-19 only)					−0.03				
					(0.14)				
(Old) Age dependency						−0.01			0.05
						(0.05)			(0.04)
Log infant mortality							1.33		−0.42
							(1.18)		(0.36)
Log health expenditure per capita								−2.48	−0.39
								(2.23)	(0.68)
First-stage F-stat	32.38	20.76	4.53	5.81	25.08	18.20	6.46	3.04	8.73
	Panel B: First Stage for *relative TIP inflow*								
Log coastline to area	0.60***	0.78***	0.24**	0.31**	1.01***	1.01***	0.57***	0.31**	0.41***
	(0.11)	(0.17)	(0.11)	(0.13)	(0.20)	(0.20)	(0.13)	(0.12)	(0.14)
	Panel C: Ordinary Least Squares								
Relative TIP flow	0.44***	0.40***	0.14**	0.16***	0.48***	0.38***	0.20***	0.07	0.14**
	(0.06)	(0.06)	(0.06)	(0.06)	(0.09)	(0.05)	(0.06)	(0.06)	(0.06)
Region dummies	Yes	Yes	Yes	Yes	Yes	Yes	Yes	Yes	Yes
Gravity controls	Yes	Yes	Yes	Yes	Yes	Yes	Yes	Yes	Yes
Countries	172	152	168	162	81	170	171	168	143
Observations	301	265	294	277	156	298	299	294	244

Notes—Panel A reports the two-stage least-squares results where the dependent variable is the log confirmed cases of the diseases, per million population, by the 3rd month into the pandemics; Panel B reports the corresponding first stages; Panel C reports the analogous OLS estimates. All regressions include the 13 region dummies, the COVID-19 dummy, and the gravity-type controls from Table III. All panels include the same set of covariates, but are not always reported in Panels B and C to conserve on space. Column (1) include the trafficking-specific institutions measure for countries compliance with the minimum standards for TIP elimination and protection services for victims. Column (2) includes the average constraint on executive measure (2000-08 and then 2010–18 for the two pandemics) from the Marshall et al. (2019) Polity data. Column (3) includes log GDP per capita. Column (4) includes other measures of government size, including size of government expenditure in relation to GDP, government health expenditure, and the *reported* numbers of tests conducted during the COVID-19 pandemic with the data coming from Max Roser, Hannah Ritchie and Hasell (2020). Column (5) includes the ratio of above-64 to working-age population. Column (6) includes log of infant mortality rate. Column (7) includes countries total health expenditure per capita. Column (8) include all the controls except for log conducted tests. Unless otherwise stated, all variables come from the World Development Indicators World Bank (2019), averaged over the years 2000–08 and 2010–18 for the H1N1 and COVID-19 pandemic, respectively. Robust standard errors in parentheses.

*** Significant at the 1 per cent level.

** Significant at the 5 per cent level.

* Significant at the 10 per cent level.

Table VI—*Social and Cultural Factors*

	(1)	(2)	(3)	(4)	(5)	(6)	(7)	(8)	(9)
	Panel A: Two-Stage Least Squares								
Relative TIP inflow	1.29***	0.99***	1.77***	1.50***	1.44***	1.54***	1.66***	1.43***	0.56**
	(0.26)	(0.20)	(0.48)	(0.48)	(0.30)	(0.29)	(0.46)	(0.30)	(0.27)
Transfers/subsidies as % of government expenses	−0.00								−0.01
	(0.01)								(0.01)
Primary school enrollment		−0.01							0.02
		(0.02)							(0.02)
Secondary school enrollment		0.04***							0.04***
		(0.01)							(0.01)
% Protestant, Muslim and Roman Catholic			0.02**						−0.01
			(0.01)						(0.00)
Ethno-linguistic fragmentation				−0.19					0.61
				(0.77)					(0.68)
Mass mobilization and protest dummy					−0.39				
					(0.53)				
Log population density						−0.11			0.22
						(0.19)			(0.15)
% population in urban areas							−0.04		0.01
							(0.03)		(0.01)
Log total fisheries production								−0.01	−0.03
								(0.06)	(0.05)
First-stage F-stat	25.30	27.75	12.39	7.74	22.75	31.44	14.00	22.94	8.02
	Panel B: First Stage for *relative TIP inflow*								
Log coastline to area	0.73***	0.71***	0.49***	0.49***	0.61***	0.71***	0.44***	0.44***	0.63***
	(0.15)	(0.13)	(0.14)	(0.17)	(0.13)	(0.13)	(0.12)	(0.12)	(0.22)
	Panel C: Ordinary Least Squares								
Relative TIP flow	0.44***	0.36***	0.45***	0.47***	0.44***	0.43***	0.29***	0.42***	0.29***
	(0.05)	(0.07)	(0.06)	(0.07)	(0.05)	(0.05)	(0.06)	(0.05)	(0.09)
Region dummies	Yes	Yes	Yes	Yes	Yes	Yes	Yes	Yes	Yes
Gravity controls	Yes	Yes	Yes	Yes	Yes	Yes	Yes	Yes	Yes
Countries	134	146	164	120	301	172	171	171	82
Observations	228	229	289	210	301	301	299	299	132

Notes—Panel A reports the two-stage least-squares results where the dependent variable is the log of confirmed cases of the diseases, per million population, by the 3rd month into the pandemics; Panel B reports the corresponding first stages; Panel C reports the analogous OLS estimates. All regressions include the 13 region dummies, the COVID-19 dummy, and the gravity-type controls from Table III. All panels include the same set of covariates, but are not always reported in Panels B and C to conserve on space. Column (1) includes the average of transfers and subsidies as a percentage of government expenses over the years 2000–08 and 2010–18 (for the H1N1 and COVID-19 pandemic, respectively). Column (2) includes the primary and secondary school net enrollment rate. Column (3) includes the percentage of the population belonging to the Roman Catholic, Muslim, and Protestant religions (1980–95), taken from La Porta et al. (1999). Column (4) includes the average of 5 ethnolinguistic fragmentation indices, taken directly from La Porta et al. (1999), originally from Easterly and Levine (1997). Column (5) includes a dummy available only for the H1N1 sample, for whether there was mass mobilization or protest in the first four months (April–July) of the H1N1 pandemic, with the data aggregated up to the country level from Clark and Regan (2016). Non-observations are imputed as zero. Column (6) includes the log of population divided by land area. Column (7) includes the percentage of population living in urban areas. Column (8) includes the total volume (metric tons) of aquatic species caught for all commercial, industrial, recreational, and subsistence purposes. Column (9) includes all the variables except for the mass mobilization dummy. Unless otherwise stated, all variables come from the World Development Indicators World Bank (2019), averaged over the years 2000–08 and 2010–18 for the H1N1 and COVID-19 pandemic, respectively. Robust standard errors in parentheses.

*** Significant at the 1 per cent level.

** Significant at the 5 per cent level.

* Significant at the 10 per cent level.

Table VII—*International Movements Factors*

	(1)	(2)	(3)	(4)	(5)	(6)	(7)	(8)	(9)
	Panel A: Two-Stage Least Squares								
Relative TIP inflow	1.39***	1.18***	1.21***	0.96***	1.05***	1.03***	1.41***	1.15***	0.74***
	(0.31)	(0.21)	(0.20)	(0.16)	(0.22)	(0.21)	(0.27)	(0.20)	(0.15)
Log migration inflow from pandemic source	−0.19**								0.02
	(0.08)								(0.05)
Log migration inflow		−0.27**							0.02
		(0.12)							(0.20)
Log of migrant stock			−0.29***						0.04
			(0.11)						(0.14)
Log of asylum-seekers inflow				−0.19***					−0.05
				(0.06)					(0.08)
Log of refugee seekers inflow					−0.16***				0.10
					(0.05)				(0.18)
Log refugee stock						−0.13**			−0.21
						(0.05)			(0.16)
Log tourist arrivals							−0.21*		−0.07
							(0.12)		(0.11)
Log tourism receipts as % of total exports								0.40***	0.26**
								(0.13)	(0.12)
First-stage F-stat	21.41	37.42	46.24	53.27	19.49	20.86	30.17	38.99	39.75
	Panel B: First Stage for *relative TIP inflow*								
Log coastline to area	0.62***	0.78***	0.79***	0.88***	0.75***	0.80***	0.63***	0.77***	0.87***
	(0.13)	(0.13)	(0.12)	(0.12)	(0.17)	(0.17)	(0.11)	(0.12)	(0.14)
First-stage F-stat									
	Panel C: Ordinary Least Squares								
Relative TIP flow	0.42***	0.43***	0.44***	0.45***	0.42***	0.41***	0.44***	0.46***	0.44***
	(0.05)	(0.05)	(0.05)	(0.06)	(0.06)	(0.05)	(0.06)	(0.05)	(0.06)
Region dummies	Yes	Yes	Yes	Yes	Yes	Yes	Yes	Yes	Yes
Gravity controls	Yes	Yes	Yes	Yes	Yes	Yes	Yes	Yes	Yes
Countries	170	170	171	148	262	160	166	162	136
Observations	298	298	298	254	262	276	288	285	232

Notes—Panel A reports the two-stage least-squares results where the dependent variable is the log of confirmed cases of the diseases, per million population, by the 3rd month into the pandemics; Panel B reports the corresponding first stages; Panel C reports the analogous OLS estimates. All regressions include the 13 region dummies, the COVID-19 dummy, and the gravity-type controls from Table III. All panels include the same set of covariates, but are not always reported in Panels B and C to conserve on space. Column (1) includes the log of migration inflow from the source country of the pandemic (Mexico for H1N1 and China for COVID-19), averaged over years 2005–10 and 2010–15, respectively. Column (2) includes log of total migration inflow. All migration flow data come from the dyadic estimates data from Abel and Cohen (2019), and averaged over years 2005–10 and 2010–15 for the H1N1 and COVID-19 pandemic, respectively. Column (3) and (6) include the log of migrant and refugee stock. Columns (4) and (5) includes the log of asylum-seekers and refugee inflow, with the data taken directly the UNHCR [United Nations High Commissioner for Refugees] (2019), for the years 2009 and 2018 for the H1N1 and COVID-19 pandemic, respectively. Columns (7) and (8) include the log of international tourist arrivals and the receipts as a % of total exports. Unless otherwise stated, all variables come from the World Development Indicators World Bank (2019), averaged over the years 2000–08 and 2010–18 for the H1N1 and COVID-19 pandemic, respectively. Robust standard errors in parentheses.

*** Significant at the 1 per cent level.

** Significant at the 5 per cent level.

* Significant at the 10 per cent level.

Table VIII—*Geography Factors*

	(1)	(2)	(3)	(4)	(5)	(6)	(7)	(8)
	Panel A: Two-Stage Least Squares							
Relative TIP inflow	1.26***	1.53***	0.74***	1.43***	1.47***	1.60***	1.27***	0.81***
	(0.34)	(0.31)	(0.22)	(0.34)	(0.33)	(0.45)	(0.28)	(0.19)
Island dummy	1.04*							−0.05
	(0.55)							(0.54)
Landlocked dummy	0.68							0.63
	(0.44)							(0.53)
Latitude		2.99*						2.04
		(1.79)						(1.92)
Land territory 100km of sea coast			2.60***					2.84***
			(0.59)					(0.63)
Mean temperature				−0.11**				−0.47
				(0.05)				(0.30)
Temperature range variables					6.36			9.91*
[ρ-value]					[0.17]			[0.08]
Humidity range variables						10.17**		14.48**
[ρ-value]						[0.04]		[0.01]
Climate/soil quality variables							10.75*	12.4*
[ρ-value]							[0.10]	[0.05]
First-stage F-stat	11.96	23.11	20.56	14.63	17.24	10.79	20.56	26.95
	Panel B: First Stage for *relative TIP inflow*							
Log coastline to area	0.53***	0.61***	1.44***	0.61***	0.63***	0.52***	0.69***	1.71***
	(0.15)	(0.13)	(0.32)	(0.16)	(0.15)	(0.16)	(0.15)	(0.33)
	Panel C: Ordinary Least Squares							
Relative TIP flow	0.39***	0.46***	0.58***	0.48***	0.45***	0.47***	0.48***	0.60***
	(0.05)	(0.05)	(0.11)	(0.06)	(0.07)	(0.07)	(0.06)	(0.14)
Region dummies	Yes	Yes	Yes	Yes	Yes	Yes	Yes	Yes
Gravity controls	Yes	Yes	Yes	Yes	Yes	Yes	Yes	Yes
Countries	172	172	59	148	148	148	148	59
Observations	301	301	104	260	260	260	260	104

Notes—Panel A reports the two-stage least-squares results where the dependent variable is the log of confirmed cases of the diseases, per million population, by the 3rd month into the pandemics; Panel B reports the corresponding first stages; Panel C reports the analogous OLS estimates. All regressions include the 13 region dummies, the COVID-19 dummy, and the gravity-type controls from Table III. All panels include the same set of covariates, but are not always reported in Panels B and C to conserve on space. Column (1) includes the dummies for whether a country is an island and is landlocked, with the data from Gurevich and Herman (2018). Column (2) includes (absolute) latitude. Column (3) includes the proportion of land territory within 100km of coastlines, from Acemoglu et al. (2001). Column (4) includes mean temperature. Column (5) includes the 4 additional temperature variables: minimum monthly low, minimum monthly high, maximum monthly low, maximum monthly high. Column (6) includes 4 humidty variables: morning minimum, morning maximum, afternoon minimum, afternoon maximum. Column (7) includes 6 dummies for soil quality (as a proxy of climate): low-latitude steppe, mid-latitude steppe, low-latitude desert, mid-latitude desert, dry steppe wasteland, and desert dry winter. Column (8) includes all the variables together. Columns (5)–(8) report the joint test of significance χ^2 and ρ-value for the temperature, humidity, and soil quality variables All temperature, humidity, and climate/soil data come directly from Acemoglu et al. (2001), originally from Parker (1997). ρ-value for joint test of significance in brackets. Robust standard errors in parentheses.

*** Significant at the 1 per cent level.

** Significant at the 5 per cent level.

* Significant at the 10 per cent level.

Table IX—*Placebo Tests for Coastline Instrument*

(1) Instrument the relative risk of TIP inflow using	(2) 2SLS estimate	(3) 2SLS estimate t-statistic
Migration inflow	-2.44	(-0.64)
Refugee inflow	-0.89	(-1.02)
Tourism arrivals	0.39	(1.28)
Refugee stock	-1.48	(-0.86)
GDP	-1.70	(-0.78)
Population living in urban areas	1.56^{***}	(3.85)
Total fisheries production	1.76	(1.07)

Notes—Each row is a 2SLS regression with the stated alternative instrument in column (1). All regressions have controls noted in the baseline 2SLS results in Table III. t-statistics are heteroskadasticity robust. *** indicates significance at the 1 per cent level.

Appendix

Table A1—*List of Country Codes and Region*

Region	ISO-3	Country	2001–11 Relative TIP inflow	Region	ISO-3	Country	2001–11 Relative TIP inflow
africa	AGO	Angola	-2.6	europe	DEU	Germany	1
africa	BDI	Burundi	-2.8	europe	DNK	Denmark	2.4
africa	BEN	Benin	-2.1	europe	ESP	Spain	2.6
africa	BFA	Burkina Faso	-2	europe	EST	Estonia	-2.4
africa	BWA	Botswana	-1.3	europe	FIN	Finland	2.3
africa	CAF	Central African Republic	-1.5	europe	FRA	France	2.9
africa	CIV	Cote d'Ivoire	2	europe	GBR	United Kingdom	2.7
africa	CMR	Cameroon	-2	europe	GEO	Georgia	-2.8
africa	COD	Congo (Kinshasa)	-2.2	europe	GRC	Greece	2.2
africa	COG	Congo (Brazzaville)	0	europe	HRV	Croatia	-0.4
africa	COM	Comoros	-3	europe	HUN	Hungary	-1.2
africa	DJI	Djibouti	-1.1	europe	IRL	Ireland	2.5
africa	DZA	Algeria	1.6	europe	ISL	Iceland	3
africa	EGY	Egypt	-1.3	europe	ITA	Italy	2.9
africa	ERI	Eritrea	-3	europe	LTU	Lithuania	-2.1
africa	ETH	Ethiopia	-3	europe	LUX	Luxembourg	2.6
africa	GAB	Gabon	3	europe	LVA	Latvia	-2.6
africa	GHA	Ghana	-2	europe	MDA	Moldova	-2.7
africa	GIN	Guinea	-2	europe	MKD	Macedonia	0.1
africa	GMB	Gambia	-2	europe	MLT	Malta	2.1
africa	GNB	Guinea-Bissau	-3	europe	MNE	Montenegro	-0.2
africa	GNQ	Equatorial Guinea	2.7	europe	NLD	Netherlands	0.8
africa	KEN	Kenya	-2	europe	NOR	Norway	2.8
africa	LBR	Liberia	-1.4	europe	POL	Poland	-1.9
africa	LBY	Libya	2.1	europe	PRT	Portugal	2.7
africa	MAR	Morocco	-2.2	europe	ROU	Romania	-2.5
africa	MDG	Madagascar	-3	europe	SRB	Serbia	-2
africa	MLI	Mali	-1.9	europe	SVK	Slovakia	-2.2
africa	MRT	Mauritania	-0.9	europe	SVN	Slovenia	0
africa	MUS	Mauritius	-2.6	europe	SWE	Sweden	2.8
africa	MWI	Malawi	-2.3	europe	UKR	Ukraine	-2.5
africa	NER	Niger	-2.1	middle_east	AFG	Afghanistan	-2.5
africa	NGA	Nigeria	-2	middle_east	ARE	United Arab Emirates	3
africa	RWA	Rwanda	-2.6	middle_east	BHR	Bahrain	3
africa	SDN	Sudan	-0.9	middle_east	IRN	Iran	-2.2
africa	SEN	Senegal	-2.1	middle_east	IRQ	Iraq	-1.3
africa	SLE	Sierra Leone	-2.2	middle_east	ISR	Israel	2.6
africa	SOM	Somalia	-2	middle_east	JOR	Jordan	2.6
africa	SYC	Seychelles	-1	middle_east	KWT	Kuwait	2.9
africa	TCD	Chad	-1.9	middle_east	LBN	Lebanon	2.3
africa	TGO	Togo	-1.7	middle_east	OMN	Oman	3
africa	TUN	Tunisia	-1.1	middle_east	QAT	Qatar	2.8
africa	TZA	Tanzania	-1.8	middle_east	SAU	Saudi Arabia	3
africa	UGA	Uganda	-2	middle_east	SYR	Syria	3
africa	ZAF	South Africa	-0.5	middle_east	YEM	Yemen	-1.4
africa	ZMB	Zambia	-2.3	north_america	CAN	Canada	0.5
africa	ZWE	Zimbabwe	-2.3	north_america	MEX	Mexico	-1.9
caribbean	ATG	Antigua and Barbuda	3	north_america	USA	US	1.4
caribbean	BHS	Bahamas	2.7	pacific	AUS	Australia	2.3
caribbean	BRB	Barbados	0.4	pacific	FJI	Fiji	-1
caribbean	CUB	Cuba	-1.7	pacific	FSM	Federated States of Micronesia	-1.7
caribbean	DOM	Dominican Republic	-2	pacific	KIR	Kiribati	-3
caribbean	HTI	Haiti	-2.2	pacific	NZL	New Zealand	1
caribbean	JAM	Jamaica	-1.6	pacific	PLW	Palau	2.5
caribbean	LCA	Saint Lucia	3	pacific	PNG	Papua New Guinea	0.6
caribbean	TTO	Trinidad and Tobago	1.7	pacific	SLB	Solomon Islands	3
caribbean	VCT	Saint Vincent and the Grenadines	-1.3	pacific	TON	Tonga	-1
central_america	BLZ	Belize	-0.4	south_america	ARG	Argentina	-0.9
central_america	CRI	Costa Rica	-0.5	south_america	BOL	Bolivia	-3
central_america	GTM	Guatemala	-2	south_america	BRA	Brazil	-1.5
central_america	HND	Honduras	-2.6	south_america	CHL	Chile	-1.9
central_america	NIC	Nicaragua	-2.7	south_america	COL	Colombia	-2.5
central_america	PAN	Panama	-1.5	south_america	ECU	Ecuador	-2
central_america	SLV	El Salvador	-2	south_america	GUY	Guyana	-2
central_asia	KGZ	Kyrgyzstan	-2.1	south_america	PER	Peru	-2.6
central_asia	TJK	Tajikistan	-3	south_america	PRY	Paraguay	-1.9
central_asia	UZB	Uzbekistan	-3	south_america	SUR	Suriname	1.7
east_asia	CHN	China	-1.9	south_america	URY	Uruguay	-2.7
east_asia	JPN	Japan	2.4	south_america	VEN	Venezuela	-1.6
east_asia	KOR	Korea, South	-1.8	south_asia	BGD	Bangladesh	-3
east_asia	MNG	Mongolia	-2.3	south_asia	IND	India	-1.5
east_asia	TWN	Taiwan	1	south_asia	LKA	Sri Lanka	-1
eurasia	KAZ	Kazakhstan	-1.6	south_asia	MDV	Maldives	3
eurasia	RUS	Russia	-2.1	south_asia	NPL	Nepal	-3
eurasia	TUR	Turkey	2.5	south_asia	PAK	Pakistan	-1.7
europe	ALB	Albania	-3	south_east_asia	BRN	Brunei	2.5
europe	ARM	Armenia	-1.9	south_east_asia	IDN	Indonesia	-2.1
europe	AUT	Austria	2.3	south_east_asia	KHM	Cambodia	-1.4
europe	AZE	Azerbaijan	-2.6	south_east_asia	LAO	Laos	-2.2
europe	BEL	Belgium	2.2	south_east_asia	MMR	Myanmar	-2.5
europe	BGR	Bulgaria	-1.9	south_east_asia	MYS	Malaysia	0.6
europe	BIH	Bosnia and Herzegovina	0	south_east_asia	PHL	Philippines	-1.9
europe	BLR	Belarus	-2.5	south_east_asia	SGP	Singapore	3
europe	CHE	Switzerland	3	south_east_asia	THA	Thailand	-1.5
europe	CYP	Cyprus	3	south_east_asia	TLS	Timor-Leste	2.8
europe	CZE	Czechia	-1.7	south_east_asia	VNM	Vietnam	-1.6

Table A2—*Data Sources and Description*

Variable	Source and Description
Relative TIP inflow; TIP standards & amnesty	Human Trafficking Indicators, 2000–11: A New Dataset Frank (2013). Relative risk of TIP (trafficking in persons) inflow Difference of (i) destination indicator, averaged 2011–11, and (ii) source indicator, averaged 2011–11.
Confirmed pandemic numbers	H1N1 sample: `https://en.wikipedia.org/wiki/2009_swine_flu_pandemic_tables` COVID-19 sample: `https://github.com/CSSEGISandData/COVID-19`
Coastline distance (km) and land area (km^2)	The World Factbook Central Intelligence Agency (2020).
Gravity-measures: Contiguity, Common language, PTA, Distance, 13 region dummies, island & landlocked dummy	The Dynamic Gravity Dataset Gurevich and Herman (2018). H1N1 sample: 2009 COVID-19 sample: 2016 (latest available) *Distance* is the population-weighted average of city-to-city bilateral distances in kilometers between each major city.
Polity measure of democracy and Constraint on Executive	Polity IV Marshall et al. (2019). H1N1 sample: 2000–08 COVID-19 sample: 2010–18 Table II: 1990–2015
Refugee and asylum-seeker flows	UNHCR [United Nations High Commissioner for Refugees] (2019) Population Statistics. H1N1 sample: 2009 COVID-19 sample: 2018 (latest available) Historical flows ratio are averaged for 1990–2005. In the data, bilateral-annual values between 1 to 4 are coded as "*" to protect anonymity of individuals, in these cases I impute * as 1.
Cocaine seizures, cocaine and amphetamine inflow	UNODC [United Nations Office on Drugs and Crimes] (2020b). Cocaine national seizures summed at country level (2012–16). Cocaine and ATS (amphetamine-type stimulants) summed at destination country (2011–16) from the Individual Drug Seizures reports.
Economic and health variables	World Development Indicators World Bank (2019). H1N1 sample: 2000–08 COVID-19 sample: 2010–18 Log GDP per capita is real GDP per capita (USD millions, constant2011); log government health expenditure per capita and log health expenditure per capita are both PPP, current international dollars); old age dependency is the ratio of above 64 to working -aged population (above 15 to 64); log population density is log of population divided by land area; log refugee stock and log migrant stock are the log of refugee population and log of international migrant stock. The World Bank (2019) data does not include Anguilla and Taiwan, so for these two cases I use the gravity data source Gurevich and Herman (2018).
Migration flows	Bilateral international migration flow estimates for 200 countries Abel and Cohen (2019). H1N1 sample: 2005–10 5–year estimates COVID-19 sample: 2010–15 5–year estimates (latest available) The migration flow estimates are the Demographic Accounting Pseudo Bayesian Closed estimates, aggregated up to destination countries. Migration inflow from pandemic source country is aggregated up to destination countries with only the pandemic source countries as inflow source.
Geography variables (temperature, humidity, soil quality, land territory 100km to coast)	Parker (1997); Acemoglu et al. (2001). Temperature variables: mean temperature, minimum monthly low, minimum monthly high, maximum monthly low, maximum monthly high. Humidity variables: morning minimum, morning maximum, afternoon minimum, afternoon maximum. Soil quality (as a proxy of climate): low-latitude steppe, mid-latitude steppe, low-latitude desert, mid-latitude desert, dry steppe wasteland, and desert dry winter.
% Protestant, Muslim, and Roman Catholic; Ethno-linguistic fragmentation	Easterly and Levine (1997); La Porta et al. (1999). Religion proportion for three most wide-spread religions in the world. Most recent of 1980–1995. Ethno-linguistic fragmentation is the average value of five different indices fractionalization of ethonolinguistic fractionalization, range 0 to 1, increasing in fragmentation. The five component indices are: (1) index of ethnolinguistic fractionalization in 1960, which measures the probability that two randomly selected people from a given country will not belong to the same ethnolinguistic group (the index is based on the number and size of population groups as distinguished by their ethnic and linguistic status); (2) probability of two randomly selected individuals speaking different languages; (3) probability of two randomly selected individuals do not speak the same language; (4) percent of the population not speaking the official language; and (5) percent of the population not speaking the most widely used language.
Mass mobilization and protest (H1N1 sample only)	Mass Mobilization Data Project, 1990–2018. Clark and Regan (2016). I filter the data to the period April–July 2009, then aggregate up the *number of participants* estimates at the country level. If this number is positive for a country in this period, the dummy is coded as 1, and 0 otherwise.
Number of tests conducted (COVID-19 sample only)	Max Roser, Hannah Ritchie and Hasell (2020) Daily recorded number of tests for countries are sporadic at the first few weeks. For each country, I use the latest available (cumulative) recorded test numbers for the day, by the end of April 2020.

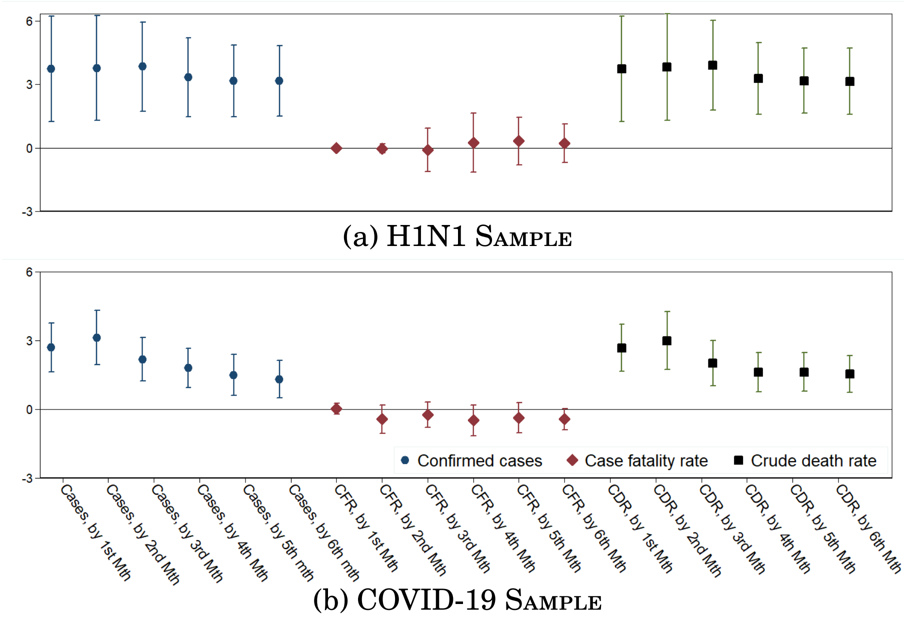

(a) H1N1 Sample

(b) COVID-19 Sample

Figure A1: 2SLS Estimates by Month (Destination Indicator)

Notes—This Figure replicates Figure IX, with the mean of destination indicator as the estimand in the structural equation (2) instead of the measure defined in equation (1). Coefficient plot of two-stage least-squares estimates with the dependent variable as cumulative confirmed numbers by the 1st to 6th month of the pandemic, and by the H1N1 and COVID-19 pandemic subsamples. All regressions control for the 13 region dummies and the gravity controls as in the specifications from Table III. The vertical bars indicate the 95 percent confidence interval constructed using the robust standard errors.

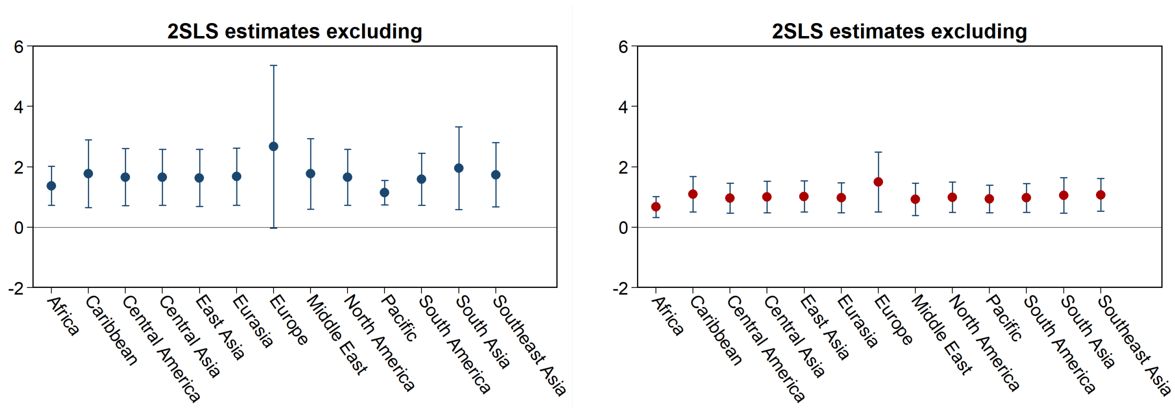

(a) H1N1 Sample (b) COVID-19 Sample

Figure A2: Regional Jackknife

Notes. Plot of the 2SLS estimate of relative TIP inflow on log confirmed cases (per million population), by the 3rd month into the pandemics, separately for the H1N1 and the COVID-19 . Each column omits countries of one of the thirteen regions in turn. The regression model is the one reported in column (4) of Table III. The vertical bars indicate 95 percent confidence interval constructed using the robust standard errors.